Elsevier Editorial System(tm) for Chemical Geology

Manuscript Draft

Manuscript Number: CHEMGE7765R1

Title: Characterising the nickel isotopic composition of organic-rich marine sediments

Article Type: Research Article

Keywords: Nickel isotope fractionation, Ni isotopes, δ60Ni, organic-rich marine sediments, Sinemurian-Pliensbachian GSSP, Exshaw Formation, redox

Corresponding Author: Dr. Sarah Porter, Ph.D.

Corresponding Author's Institution: Chemostrat Ltd

First Author: Sarah Porter, Ph.D.

Order of Authors: Sarah Porter, Ph.D.; David Selby; Vyllinniskii Cameron

Abstract: New Ni stable isotope data (δ60Ni) determined by double-spike MC-ICP-MS for two geologically distinct suites of organic-rich marine sediments from the Sinemurian-Pliensbachian (S-P) Global Stratotype Section and Point (GSSP (; Robin Hood's Bay, UK) and the Devonian-Mississippian Exshaw Formation (West Canada Sedimentary Basin) is presented herein. These sediments yield δ60Ni values of between 0.2 ‰ and 2.5 ‰, and predominantly have Ni isotopic compositions that are heavier than those of abiotic terrestrial and extraterrestrial samples extraterrestrial and abiotic terrestrial samples (-0.1 ‰ and 0.4 ‰)(0.15 ‰ and 0.27 ‰), and in some cases present-day seawater (1.44 ‰) and dissolved Ni from riverine input (0.80 ‰). In addition, the observed degree of isotopic fractionation in the marine sediments is far greater than that of these other sample matrices. However, a strong similarity is exhibited between the δ60Ni values of the organic-rich sediments studied here and those of ferromanganese crusts (0.9 to 2.5 ‰), suggesting that factors ubiquitous to the marine environment are likely to play a key role in the heightened level of isotopic fractionation in these sample matrices.

A lack of correlation between the Ni stable isotope compositions of the organic-rich sediments and Ni abundance, suggests that isotopic fractionation in these sediments is not controlled by uptake incorporation or enrichment of Ni during sediment accumulation. Further, no relationship is observed between δ60Ni and TOC concentrations or bottom-water redox conditions, indicating that the organic carbon reservoir and levels of oxygenation at the sediment-water interface do not exert a primary control on Ni isotope fractionation in marine sediments. Following examination of these relationships, it is therefore more likely that the heavy Ni isotope compositions of marine sediments are controlled by the weathering environment and the dominant sources of dissolved Ni into the global ocean reservoir.

Characterising the nickel isotopic composition of organic-rich marine sediments

Sarah J. Porter[1,2*], David Selby[1], and Vyllinniskii Cameron[3]

[1] Department of Earth Sciences, Science Labs, Durham University, Durham, DH1 3LE, UK
[2] Chemostrat Ltd., Unit 1 Ravenscroft Court, Buttington Cross Enterprise Park, Welshpool, Powys, SY21 8SL, UK
[3] Bristol Isotope Group, School of Earth Sciences, University of Bristol, Bristol BS8 1RJ, UK

[*]Corresponding author: Sarah J. Porter. Email: sarahporter@chemostrat.com; Tel.:+44(7889)838599

Keywords: Nickel isotope fractionation, Ni isotopes, δ^{60}Ni, organic-rich marine sediments, Sinemurian-Pliensbachian GSSP, Exshaw Formation, redox

Abstract

New Ni stable isotope data (δ^{60}Ni) determined by double-spike MC-ICP-MS for two geologically distinct suites of organic-rich marine sediments from the Sinemurian-Pliensbachian (S-P) Global Stratotype Section and Point (GSSP ~~(~~; Robin Hood's Bay, UK) and the Devonian-Mississippian Exshaw Formation (West Canada Sedimentary Basin) is presented herein. These sediments yield δ^{60}Ni values of between 0.2 ‰ and 2.5 ‰, and predominantly have Ni isotopic compositions that are heavier than those of abiotic terrestrial and extraterrestrial samples ~~extraterrestrial and abiotic terrestrial samples (-0.1 ‰ and 0.4 ‰)~~(0.15 ‰ and 0.27 ‰), and in some cases present-day seawater (1.44 ‰) and dissolved Ni from riverine input (0.80 ‰). In addition, the observed degree of isotopic fractionation in the marine sediments is far greater than that of these other sample matrices. However, a strong similarity is exhibited between the δ^{60}Ni values of the organic-rich sediments studied here and those of ferromanganese crusts (0.9 to 2.5 ‰), suggesting that factors ubiquitous to

the marine environment are likely to play a key role in the heightened level of isotopic fractionation in these sample matrices.

A lack of correlation between the Ni stable isotope compositions of the organic-rich sediments and Ni abundance, suggests that isotopic fractionation in these sediments is not controlled by ~~uptake~~ incorporation or enrichment of Ni during sediment accumulation. Further, no relationship is observed between δ^{60}Ni and TOC concentrations or bottom-water redox conditions, indicating that the organic carbon reservoir and levels of oxygenation at the sediment-water interface do not exert a primary control on Ni isotope fractionation in marine sediments. Following examination of these relationships, it is therefore more likely that the heavy Ni isotope compositions of marine sediments are controlled by the weathering environment and the dominant sources of dissolved Ni into the global ocean reservoir.

1. Introduction

For several decades previous investigations of Ni isotopes have focused predominantly on characterising radiogenic isotopic fractionation in extraterrestrial materials, with a view to enhancing our understanding of planetary processes and the isotopic composition of the early Solar System (eg. Kohman and Robison, 1980; Morand and ~~Allegre~~Allègre, 1983; Shimamura and Lugmair, 1983; Birck and Lugmair, 1988; Herzog et al., 1994; Xue et al., 1995; Quitté et al., 2006; Cook et al., 2007; Moynier et al., 2007; Chen et al., 2009). Further, the role of Ni as a bioessential trace metal (eg. Frausto da Silva and Williams, 2001; Cameron et al., 2007; 2009) has led to the recognition that the stable isotopes of Ni may have the potential to be utilised as a powerful biological tool for studies of early life on Earth (Cameron et al., 2009; 2012).

In addition to its role in cosmochemical and biochemical investigations, the potential of Ni to significantly enhance our understanding of organic-rich sedimentary environments and to provide a powerful geological tracer in the petroleum realm has been recognised, following pioneering work by Lewan and Maynard (1982) and Lewan (1984) (eg. Ellrich et al., 1985; Manning et al., 1991; Alberdi and Lafargue, 1993; López et al., 1995). However, these studies focused on the elemental distribution of Ni rather than on its isotopic characterisation, and as such, no study currently exists that evaluates the behaviour of Ni stable isotopes in

82 organic-rich sediments or indeed within a stratigraphic profile. This can be attributed
83 to Ni being a relatively newly investigated system, together with the difficulty
84 associated with purifying Ni from such complex sample matrices, that has only
85 recently been overcome through advancements in analytical and mass spectrometry
86 techniques (eg. Gall et al., 2012; Cameron and Vance, 2014).
87 Until now, Ni stable isotope systematics in organic-rich sedimentary matrices
88 have not been investigated. Indeed, it is only recently that the Ni isotopic
89 composition of seawater and the sources of Ni to the global oceanic reservoir have
90 been determined (e.g. Cameron and Vance, 2014; Gall et al., 2013). Present-day
91 seawater has an average δ^{60}Ni value of 1.44 ± 0.15 ‰, with apparent global isotopic
92 homogeneity (Cameron and Vance, 2014). The oceanic residence time of Ni has been
93 calculated as ~30 kyr (Cameron and Vance, 2014), which is significantly longer than
94 the mixing time of the global oceans (~2,000 yrs; Palmer et al., 1988). This would be
95 sufficient for the ocean to have an isotopically homogenous Ni composition.
96 Cameron et al. (2014) also demonstrate that draw-down of Ni from the surface to
97 deep ocean during trace metal cycling is not accompanied by isotopic fractionation,
98 thus further suggesting that the ~~global~~modern ocean is isotopically homogenous. In
99 the absence of any Ni isotope studies on banded iron formation and shale datasets,
100 it is difficult to speculate on processes occurring in an ancient ocean. However,
101 examination of Ni/Fe data from banded iron formations and extrapolated maximum
102 dissolved Ni concentration values in sea water through time (Konhauser et al., 2009),
103 demonstrates that dissolved nickel concentrations may have reached present day
104 values by ~550 Ma. As such, given the age of the sediments being studied herein
105 (~190-360 Ma), it is appropriate to use what we know regarding modern ocean

circulation and fractionation processes to hypothesise about processes acting in the ancient oceans.

The predominant input of dissolved Ni to the oceans occurs via riverine influx, which has been suggested to yield an annual discharge- and concentration-weighted δ^{60}Ni average of +0.80 ‰ (Cameron and Vance, 2014). Significant variability in the riverine isotopic composition has been observed (+0.29 to +1.34 ‰), which has been attributed to isotopic fractionation of Ni during weathering of continental crust, resulting in heavier δ^{60}Ni values in rivers and seawater. In addition, mineral dust and volcanic ash also contribute to the oceanic Ni budget (Li and Schoonmaker, 2003), as well as hydrothermal vent fluids (δ^{60}Ni = 1.5 ‰; Gall et al., 2012).

Herein we present the first attempt at creating a Ni isotope stratigraphic profile for an organic-rich sedimentary succession. The marine section across the Sinemurian-Pliensbachian Global Stratotype Section and Point (GSSP), Robin Hood's Bay, UK, is ideally suited to the present study, as it well understood biostratigraphically (Hesselbo et al., 2000; Meister et al., 2006) and has been previously characterised using other isotope stratigraphy techniques, including strontium (^{87}Sr/^{86}Sr; Jones et al., 1994; Hesselbo et al., 2000), oxygen (δ^{18}O), carbon (δ^{13}C) (Hesselbo et al., 2000), and Re-Os isotopes (Porter et al., 2013). The section is also consistently thermally immature (the rocks have not been subjected to enough heat or pressure to convert any kerogens present to hydrocarbons), thereby eliminating any potential effects of thermal maturation on the Ni isotope signature. In addition, to draw comparison between the isotopic composition of samples of different depositional ages and environments, we present Ni isotope data from a

selection of thermally immature black shale samples from a core of the Exshaw Formation, Canada.

To accurately assess and interpret any stratigraphic variation of Ni isotopes in the Robin Hood's Bay section and Exshaw Formation samples, it is critical to determine whether any fluctuations in paleoredox conditions occur. Nickel primarily occupies one oxidation state in the natural environment (Ni^{2+}), suggesting that it is not redox sensitive. However, its preferential association with redox-sensitive metallo-organic complexes (porphyrins) in organic-rich sediments (Lewan and Maynard, 1982) indicates that certainly within these sample matrices, redox conditions at the time of sediment deposition may directly impact the degree of enrichment or depletion of Ni. Herein, paleoredox conditions have been established for the Sinemurian-Pliensbachian GSSP section and the Exshaw Formation sample suite. Although one previous study (Dewaker et al., 2000) provides a preliminary dataset for the Ni isotope composition of sediments from 3 different basins, our understanding of the behaviour of Ni isotope systematics within organic-rich sediments is currently non-existent. Further, advancements in analytical techniques over the past decade suggest that the methodology employed by Dewaker et al. (2000) may not have been optimal for Ni separation or Ni stable isotope analysis.

This paper presents the first detailed study of nickel stable isotope systematics in organic-rich marine sediments. Analysis of marine sediments of different depositional ages and from two geologically distinct settings, the Sinemurian-Pliensbachian boundary (UK) and the Devonian-Mississippian Exshaw Formation (Canada), yields comparable Ni isotope compositional values for both sites. These samples provide insight into the incorporation~~uptake~~ of Ni into ocean

sediments, and allow evaluation of the contribution of the various dissolved Ni fluxes to the seawater during these time periods.

2. Geological Setting

2.1 The Sinemurian-Pliensbachian boundary GSSP, Robin Hood's Bay, UK

The Sinemurian-Pliensbachian boundary, established from the succession's complete ammonite assemblages (Spath, 1923; Dean et al., 1961; Hesselbo et al., 2000; Meister et al., 2006), occurs in the Pyritous Shales of the Redcar Mudstone Formation within the Lias Group at Robin Hood's Bay (Powell, 1984; Fig. 1). At this point in the Early Jurassic, Robin Hood's Bay was positioned on the margins of a shallow epicontinental sea (eg. Dera et al., 2009) that covered most of Northern Europe, including Britain, during the Mesozoic (Sellwood and Jenkyns, 1975). The facies changes across the boundary, from pale siliceous to finer, more organic-rich mudstones (Fig. 2), indicate an overall relative increase in sea level of at least regional extent (~~eg.,~~eg. Hesselbo et al., 2000; Meister et al., 2006; Porter et al., 2013).

The age for the base of the Pliensbachian has been defined by the Geological Time Scale (GTS) 2012 as 189.6 ± 1.5 Ma (Gradstein et al., 2012), derived from cycle-scaled linear Sr trends and ammonite occurrences (as noted above; also includes the lowest occurrence of *Bifericeras donovani*; Gradstein et al., 2012).

2.2 Exshaw Formation, West Canada Sedimentary Basin (WCSB)

178 The West Canada Sedimentary Basin (WCSB) trends approximately NW-SE
179 between the Canadian Shield to the East and the Western Cordillera to the West
180 (Piggott and Lines, 1992). Within the WCSB lies the Exshaw Formation, a thin but
181 laterally continuous unit (2-12 m thick; Leenheer, 1984; Creaney and Allan, 1991).
182 The Exshaw Formation in south-west and western Alberta (Fig. 3) comprises a lower
183 member of organic-rich mudrocks and black shales which rest with minor
184 disconformity upon Upper Devonian carbonate strata (Richards et al*.,* 1999), and are
185 abruptly to gradationally overlain by bioturbated shelf siltstones (Caplan and Bustin,
186 1998, 1999; Creaser et al*.,* 2002). The depositional interval of the lower black shale
187 unit is well constrained biostratigraphically; between the *expansa* and *duplicata*
188 zones of Late Famennian to Early Tournaisian time (over a maximum time period of
189 ~363 – 360 Ma; Caplan and Bustin, 1998). These lower black shales are dark grey,
190 bituminous, relatively thin (consistently between 3-5 m; Meijer et al*.,* 1994) and
191 widespread (Meijer et al*.,* 1994). The Devonian-Mississippian boundary (Exshaw-type
192 section at Jura Creek, ~80 km west of Calgary, Alberta, Canada) represents the
193 boundary between the upper calcareous and lower non-calcareous black shale units
194 (Richards and Higgins, 1988). Selby and Creaser (2005) provide an absolute Model 1
195 Re-Os age for this boundary, and thus the top of the lower black shale unit, of 361.3
196 ± 2.4 Ma. In addition, U-Pb monazite data from a tuff horizon close to the base of the
197 lower black shale member constrains an absolute depositional age for this unit of
198 363.4 ± 0.4 Ma (Richards et al*.,* 2002). Deposition at this time represents part of a
199 continent-wide Famennian-Tournaisian black shale event, and in turn, a possible
200 ocean anoxic event (Piggott and Lines, 1992).
201

3. Sampling

A set of 32 samples (SP7-09 to SP39-09) was collected from the Pyritous Shales Member of the Redcar Mudstone Formation, along a 6 m vertical section bracketing the Sinemurian–Pliensbachian boundary (sample SP22-09) at Robin Hood's Bay (Fig. 2). This marine sequence contains a rich fauna of ammonites both above and below the boundary interval (Hesselbo et al., 2000). Total organic carbon analysis was conducted on all samples, with a consistent sampling interval of ~20 cm for 3 m above and 3 m below the boundary from Beds 69–75 (except within Bed 72, where a smaller sampling interval of ~15 cm was used). Of these samples, 14 were analysed for Ni isotopes at a sampling interval of ~40 cm (Fig. 2).

Four samples from the Lower member of the Exshaw Formation were collected from the Alberta Energy and Utilities Board, Core Research Centre, Calgary (Fig. 3). The samples were taken from core 3-19-80-23W5, as detailed in Piggot and Lines (1992) and Creaser et al. (2002). All samples are thermally immature, fine-grained black shales containing very thin parallel and undulating laminations, and showing no evidence of post-depositional disturbance. Drill core samples were obtained to avoid any potential effects of surface weathering, including loss of organic matter (Peucker-Ehrenbrink and Hannigan, 2000). Further, edges of the core were polished and where possible samples were taken from the central part of the core.

4. Analytical Protocol

4.1 Trace element abundance and TOC

The elements V, Cr, Ni and Co were analysed in this study in order to look at relative changes of depositional redox conditions in the sediments of interest. Samples were prepared for trace element analysis at the Durham Geochemistry Group (University of Durham, UK) following the method of Ottley et al., (2003). Sample powders (~100 mg) were digested in a 4:1 solution of 29 N HF and 16 N HNO_3 at ~150 ^{o}C for 48 hrs. Samples were then evaporated to near rather than total dryness, to avoid stabilisation of insoluble fluorides (Ottley et al., 2003). This was followed by the addition of 1 ml 16 N HNO_3 and evaporation to near dryness. The previous stage was repeated before the addition of 2.5 ml 16 N HNO_3 and ~10 ml 18MΩ water to create a ~4 N HNO_3 solution. Sample beakers were capped and heated on the hotplate overnight at ~100 ^{o}C. Once cooled, 1 ml of 1 ppm internal Re and Rh spike was added to the samples (to yield 20 ppb Re and Rh in the final analyte solution) before dilution up to 50 ml with MQ, yielding a ~0.5 N HNO_3 solution. Prior to analysis, samples were diluted 10-fold by taking 1 ml from the 50 ml solution and diluting it to 10 ml using 0.5 N HNO_3. Samples were then analysed using the Thermo X-Series Quadrupole Inductively Coupled Plasma Mass Spectrometer (ICP-MS).

~~———~~Replicate analyses of USGS International Reference Materials (RMs) AGV-1, BHVO-1 and W-2 ~~and synthetic standards solutions for Mo (10, 20 and 30 ppb solutions)~~ were conducted for calibration per sample set.

Total organic carbon measurements were performed at Durham University using a Costech Elemental Analyser (ECS 4010) coupled to a ThermoFinnigan Delta V Advantage. Total organic carbon was obtained as part of the isotopic analysis ($\delta^{13}C_{org}$) using an internal standard (Glutamic Acid, 40.82 % C). Data accuracy was monitored through routine analyses of in-house standards, which are stringently calibrated against international standards (eg. USGS 40, USGS 24, IAEA 600, IAEA CH6).

4.2 Nickel stable isotopes

All Ni isotope analyses were conducted at the University of Bristol. Samples (~100 mg) were digested in closed PFA Beakers (Savillex, Minnetonka, MN) in a mixture of concentrated HF and HNO_3 (3:1) at 140 ^{o}C for 48 hrs. Dried samples were treated further with 7 N HCl. Chemical separation, purification and analyses of Ni isotopes was carried out as described in detail in Cameron et al. (2009) and Cameron and Vance (2014)~~, 2013)~~. Briefly, sample aliquots were spiked and allowed to equilibrate under heating in closed vials overnight. This was followed by drying down and treatment with 7 N HCl + H_2O_2. The spiked samples were then put through a 3-stage column procedure that in turn removes Fe and Zn, separates Ni from the bulk sample matrix, and final purification to remove any residual Fe and Zn. The first ion-exchange column (AG MP-1M, Bio-Rad) is used to remove Fe and Zn. The dried samples are then taken up in 1M HCl/1 M ammonium citrate, and the pH adjusted to 8–9 before loading onto columns filled with Ni resin (Eichrom Technologies). This step separates Ni while removing all other matrix elements in the sample. After oxidation to remove Ni-bound DMG, the samples are finally put through a third

column, which is a repeat of the first anion column, to clean up any residual Fe and Zn.

All analyses were conducted in low resolution mode using a ThermoFinnigan Neptune multi-collector (MC) ICP-MS coupled to an Aridus desolvating nebuliser system (CETAC, Omaha, NE, USA). Samples were introduced in 2% HNO_3 via a CPI PFA nebuliser (50 μl/minute) and spray chamber. Prior to isotopic analysis, the $^{56}Fe/^{58}Ni$ ratio was manually checked in high resolution mode in all samples so that any potential isobaric interference from residual sample ^{58}Fe could be applied as a correction to Ni mass 58. Relative to the propagated internal uncertainty on $\delta^{60}Ni$, the correction was insignificant. Additionally, a small amount of N_2 was introduced to the Aridus sweep gas to reduce a potential interference from $^{40}Ar^{18}O$ at mass 58. To mitigate inaccuracies in the $\delta^{60}Ni$ brought on by any instrumental variations, measurements of the pure NIST SRM986 standard were made throughout the analytical session. The reproducibility and accuracy of all isotope ratios were monitored further by measurement of mixtures of the SRM986 standard with the double-spike. All isotopes were measured simultaneously in static mode using a multiple Faraday collector array. All Ni data are reported relative to NIST SRM986, in the standard delta notation ($\delta^{60}Ni = [(^{60}Ni/^{58}Ni)_{sample}/(^{60}Ni/^{58}Ni)_{NISTSRM986})-1] \times 1000$), with all uncertainties reported to the 2σ level.

5. Results

5.1 Trace elements and TOC

296 The trace element ratios Ni/Co, V/Cr and V/(V+Ni) have been utilised by
297 previous studies to evaluate paleoredox conditions at the time of sediment
298 deposition (eg. Hatch and Leventhal, 1992; Jones and Manning, 1994; Schovsbo,
299 2001; Rimmer, 2004). Both Ni and V occur in highly stable tetrapyrrole complexes
300 that are originally derived from chlorophyll and are preferentially preserved under
301 anoxic conditions (Lewan and Maynard, 1982). When organic matter has been
302 extensively exposed to aerobic conditions, preservation of these tetrapyrrole
303 complexes will be low and subsequently the organic matter will have low Ni and V
304 contents. Chromium is not influenced by redox conditions, and thus because of its
305 association with just the detrital fraction and not the organic matter (Dill, 1986), high
306 V/Cr values (>2) are indicative of anoxic conditions. Both Ni and Co are found in
307 pyrite (in addition to the occurrence of Ni in porphyrins), but high Ni/Co values are
308 associated with anoxic conditions (Jones and Manning, 1994). The relationship
309 between these ratios and depositional redox conditions are summarised in Table 1.
310 The abundances of Ni, Co, V, Cr and TOC for all samples from Robin Hood's
311 Bay and the Exshaw Formation, are presented in Table 2. Both the Ni/Co and V/Cr
312 indices for Robin Hood's Bay show that these sediments were deposited under
313 predominantly oxic conditions. ~~Good agreement is observed between both the~~
314 ~~Ni/Co and V/Cr indices for Robin Hood's Bay, which show that the samples were~~
315 ~~deposited under predominantly oxic conditions.~~ However, there is significant
316 disagreement between these ratios and the V/(V+Ni) index. Values for V/(V+Ni)
317 range from ~0.51 – 0.89 and indicate that anoxic conditions prevailed across the
318 Sinemurian-Pliensbachian boundary. Further, six samples suggest that bottom-water

circulation ceased and that conditions became euxinic intermittently between ~2.6 m above the boundary and ~1.9 m below it (Table 2).

The Ni/Co ratio in the Exshaw Formation sediments ranges from 13.8 – 21.4, with all four samples falling within the suboxic-anoxic parameter (Table 2). Similarly, the V/(V+Ni) ratio indicates that three of the samples were deposited under suboxic-anoxic conditions (SP8-10, SP10-10 and SP13-10; values of 0.67, 0.69 and 0.67, respectively). However, whilst V/Cr values of 7.2 and 9.0 suggest a suboxic-anoxic depositional environment for Exshaw Formation samples SP10-10 and SP13-10, respectively, this ratio also yields values that are representative of dysoxic conditions for samples SP8-10 and SP9-10 (2.0 and 2.1, respectively).

Total organic carbon content is generally low in the Sinemurian-Pliensbachian sediments, varying from ~0.53 – 2.46 wt. % (Table 2; Fig. 4). The data shows only slight variation prior to the boundary (~0.57 – 0.86 wt. %; Fig. 4), but an overall gradual increase above the boundary (from ~0.58 – 2.46 wt. %; Fig. 4). Total organic carbon values in the Exshaw Formation samples range from 1.2 – 11 wt. %.

5.2 Nickel stable isotopes

New Ni stable isotope data for a select suite of the organic-rich sediments at Robin Hood's Bay is presented (see Table 3). From the base of Bed 71 the sampling interval for Ni isotope analysis is ~40 cm (Fig. 2). A profile of δ^{60}Ni values for the section is shown alongside Ni concentration and TOC for comparison (Fig. 4).

The δ^{60}Ni of these samples is extremely variable, ranging from 0.28 ± 0.05 – 1.60 ± 0.05 ‰ (Fig. 4; Table 3). Two noticeable peaks in δ^{60}Ni values are observed 0.8 m above and 2.1 m below the Sinemurian-Pliensbachian boundary (1.26 ± 0.05 ‰

343 and 1.60 ± 0.05 ‰, respectively) that approximately correlate with the tops of beds
344 70 and 74. The greatest range in δ^{60}Ni values occurs below the boundary (~1.32 ‰),
345 compared to a range of ~0.97 ‰ above the boundary (Fig. 4). In this section and
346 dataset there is no apparent relationship between the degree of Ni isotope
347 fractionation and depositional redox conditions, TOC or stratigraphic height (Fig. 4).
348 Nickel stable isotope data for the Exshaw Formation is also presented in
349 Table 3. The δ^{60}Ni values in these samples range from 0.46 ± 0.04 to 2.50 ± 0.04 ‰
350 (Table 3). As with the Robin Hood's Bay section, no relationship exists between δ^{60}Ni
351 and sample depth or between δ^{60}Ni and depositional redox conditions, TOC or
352 stratigraphic position (Fig. 4).
353
354
355 **6. Discussion**
356
357 *6.1. Evaluating the suitability of V/(V+Ni) as a redox proxy: How applicable is it?*
358 The Ni/Co and V/Cr redox indices are recommended by a number of workers
359 as the most reliable of the paleo-environmental proxies (eg. Jones and Manning,
360 1994; Rimmer, 2004), and have been used by several studies to provide accurate and
361 consistent evaluations of paleoredox conditions at the time of sediment deposition
362 (eg. Rimmer, 2004; Selby et al., 2009; this study). However, this study finds that
363 there is significant disagreement between these indices and the V/(V+Ni) index. For
364 Robin Hood's Bay, the latter index suggests that the sediments were deposited in
365 predominantly suboxic-anoxic bottom-waters, with intermittent euxinic periods.
366 However, both the V/Cr and Ni/Co ratios indicate that the Robin Hood's Bay samples

were deposited under largely oxic condition. Such disparity between the redox indices is also noted by both Rimmer (2004) and Selby et al. (2009), who observe that the V/(V+Ni) index suggests suboxic-anoxic conditions for sediments otherwise indicated to have been deposited under oxic conditions by the V/Cr and Ni/Co ratios.

Preliminary work by Lewan and Maynard (1982) and Lewan (1984) suggested that redox potential was a dominant control on the wide range of V/(V+Ni) values observed in petroleum source rocks and oils. Following this, Hatch and Leventhal (1992) were the first to develop and utilise the V/(V+Ni) index as a measure of relative redox potential in organic-rich sediments. Their study focused on applying this index specifically to marine black shales in the Pennsylvanian Stark Shale Member of the Dennis Limestone, Wabaunsee County, Kansas, USA (Hatch and Leventhal, 1992). Therefore, the ranges they defined for the V/(V+Ni) ratio and the associated redox conditions (summarised in Table 1), are applicable to this specific geological basin and are sensitive to localised geochemical variations therein.

Hatch and Leventhal (1992) show that for the Stark Shale Member, with the exception of two outliers, low TOC values (<2.5 wt. %) correspond to V/(V+Ni) values <0.75, and samples containing greater TOC (>7.5 wt. %) have corresponding higher V/(V+Ni) values (0.75; Fig. 5). However, this relationship is not observed in the majority of the Sinemurian-Pliensbachian or Exshaw Formation sediments, with samples containing low TOC providing a range in V/(V+Ni) data from ~0.33 – 0.89. This immediately indicates that there are significant geochemical differences between these three geological sites. ~~have differing geochemical frameworks.~~ This may be due to differences in both geological age and stratigraphy, with the Stark Shale Member (Late Carboniferous) being a darker grey, non-sandy shale with higher

391 TOC content (Hatch and Leventhal, 1992). As such, this comparison suggests that the
392 redox index V/(V+Ni), originally developed for a specific geological basin, may not be
393 applicable to other geological sites, particularly those that possess differing
394 geological and geochemical characteristics. Factors that may have a profound effect
395 upon the applicability of such a threshold from one study to another include:
396 differences in the influx of nutrients and trace elements, type and relative amounts
397 of organic matter, and degrees of oceanic mixing (~~eg.,~~eg. Rimmer, 2004). However,
398 these are preliminary findings from a small dataset and further investigation is
399 recommended. In agreement with Rimmer (2004), this study therefore suggests that
400 caution should be taken when applying redox indices established by other studies for
401 ~~specific~~ single geological sites.
402
403 *6.2. Nickel stable isotope fractionation in marine sediments*
404 Nickel stable isotope data for the Exshaw Formation and the Sinemurian-
405 Pliensbachian GSSP is presented in Table 3 and Figure 6, and is the first to be
406 obtained for a suite of organic-rich marine sediments. The Exshaw Formation shales
407 define a realm of δ^{60}Ni values of 0.46 ± 0.04 to 2.50 ± 0.04 ‰ (a range of ~2.04 ‰;
408 Fig. 6). This range overlaps with, and is comparable to the δ^{60}Ni data for the
409 Sinemurian-Pliensbachian boundary GSSP (0.28 ± 0.05 to 1.60 ± 0.05 ‰; ~1.32 ‰;
410 Fig. 6). Although there are currently no estimations for the Ni isotopic composition
411 of the palaeo-ocean, the present-day global seawater δ^{60}Ni value has been
412 constrained as 1.44 ± 0.15 ‰ (Cameron and Vance, 2014). This value lies within the
413 δ^{60}Ni range of the marine sediments (Fig. 6; this study). Draw-down of Ni through
414 the water column does not induce isotopic fractionation, and as such, the Ni stable

isotope composition of the ocean is assumed to be homogenous (Cameron and Vance, 2014). However, the Ni stable isotope composition of the organic-rich sediments is far from homogenous, with δ^{60}Ni values that are either significantly lighter or heavier than the present-day seawater δ^{60}Ni value (Fig. 6). Assuming that global ocean homogeneity has persisted throughout geological time, the fractionation observed in the marine sediments must therefore be recording the substantially variable isotopic compositions of the sources of dissolved Ni into the oceans.

This preliminary study presents Ni isotope and Ni concentration data from bulk sample analysis. To assess what fraction of the selected metals may be authigenic versus lithogenic, Table 4 presents Ni concentration data from this study, and from average shale and average upper continental crust. It is clear from this that the authigenic contribution of Ni in these samples is < 50 % (Table 4), suggesting that > 50 % of the sample is represented by the lithogenic fraction.

For both sample sets, no correlation is observed between δ^{60}Ni and Ni abundance, indicating that the level of Ni isotope fractionation in bulk~~the~~ marine sediments here is not directly controlled by the degree of Ni enrichment. -Similarly, no relationship exists between δ^{60}Ni and redox for either sample set, suggesting that the level of isotopic fractionation is not solely dictated by the bottom water redox conditions at the time of sediment deposition. However, although it is currently poorly understood, it is interesting to consider whether or not the degree of organic matter preservation could have an effect on the observed isotopic fractionation within the sediments. The samples used for Ni isotope analysis across the Sinemurian-Pliensbachian boundary were deposited in predominantly oxic

conditions (using the Ni/Co and V/Cr ratios). The tetrapyrrole complexes known to hold the majority of ~~the~~ Ni in organic matter are poorly preserved under these conditions (Lewan and Maynard, 1982). As such, assuming break down of these complexes is heterogeneous, and that it does not result in the preferential loss of a particular isotope of Ni, this lack of preservation may at least partially contribute to the observed Ni isotope fractionation in these sediments.

In addition, no correlation is seen between δ^{60}Ni and TOC concentration in these samples, indicating that Ni isotope fractionation is not dependent on the concentration of organic matter in these sediments. However, all samples in this study have TOC contents of <3.0 wt. % (Table 3; apart from Exshaw Fm. sample SP10-10; 11.05 wt. %). As such, to further investigate the relationship between Ni fractionation and the organic carbon reservoir, work should be conducted on samples containing more varied and greater levels of TOC.

6.3. Fractionation of nickel stable isotopes in marine organic-rich sediments vs. terrestrial samples, extra-terrestrial samples and ferromanganese crusts

Marine sediments from the Exshaw Formation and Sinemurian-Pliensbachian GSSP yield a comparable range in δ^{60}Ni values (0.5-2.5 ‰ and 0.3-1.6 ‰, respectively; Fig. 6). Figure 6 compares these Ni isotopic values with that of bulk Earth and extraterrestrial samples (Cameron et al., 2009), including meteorites (0.2 ‰ to 0.4 ‰), basalts (0 to 0.3 ‰) and continental sediments (0 to 0.2 ‰). It is clear that these samples are significantly isotopically lighter than the organic-rich sediments (this study). In addition, Ni stable isotope fractionation occurs to a much greater degree in the sedimentary marine environment. Despite this though, there is

463 minimal overlap between the δ^{60}Ni values for the organic-rich sediments and those
464 of the abiotic terrestrial and extraterrestrial samples (Fig. 6).

465 The reasons for the heightened isotopic fractionation in marine sediments
466 are currently poorly understood due to an extremely limited sample database.
467 However, the complexity of the marine environment is likely to play a critical role in
468 this. With assumed ocean isotopic homogeneity (Cameron and Vance, 2014), the
469 sources of dissolved Ni into seawater must exert a substantial control on the
470 observed degree of isotopic fractionation. This may be partially attributed to the
471 variability of the Ni isotope composition of the dissolved phase of rivers, which are a
472 dominant source of Ni to the global oceans (δ^{60}Ni = 0.29 to 1.34 ‰; Cameron and
473 Vance, 2014). The heavier isotope composition of this fraction relative to silicates
474 and continental sediments (0 ‰ to 0.3 ‰; Cameron et al., 2009) likely reflects
475 isotopic fractionation induced by the weathering environment during riverine
476 transport (Cameron and Vance, 2014).

477 However, this study demonstrates that the Ni isotopic composition of
478 organic-rich marine sediments (δ^{60}Ni = 0.28 to 2.50 ‰; this study) are significantly
479 heavier than that of the riverine source (average δ^{60}Ni = 0.80 ‰; Cameron and
480 Vance, 2014). This is also the case for the dissolved phase of present-day seawater
481 (δ^{60}Ni = 1.44 ± 0.15 ‰; Cameron and Vance, 2014). To reconcile this, there must
482 therefore be either an additional input that is isotopically heavier than the riverine
483 source (Cameron and Vance, 2014).

484 Dissolved trace metals are often removed from the water column via
485 adsorption to mineral surfaces as they are incorporated into the sediment. The
486 adsorption process, in particular to Mn and Fe oxyhydroxides, is known to induce

isotopic fraction in a number of stable isotope systems, including Mo and U (Brennecka et al., 2011; Wasylenki et al., 2008; 2011). Sorption to Fe-Mn oxides is the main output of Ni from the oceans (Cameron and Vance, 2014), and more recently, this fractionation effect has also been revealed in the Ni stable isotope system (Wasylenki et al., 2014). In addition, experiments focusing on the adsorption and co-precipitation of Ni with oxyhydroxide phases (Wasylenki et al., 2014) have demonstrated that isotopically light Ni is retained by these phases whilst isotopically heavy Ni is mobilised. This therefore leads to an enrichment of isotopically heavy Ni in the dissolved riverine load (Wasylenki et al., 2014).

~~Further,~~ Nickel stable isotope data for ferromanganese crusts (0.9-2.5 ‰; Gall et al., 2013) shows that their isotopic composition is comparable to that of the marine organic-rich sediments discussed herein. Following analysis of ferromanganese crusts in proximity to hydrothermal sources, Gall et al. (2013) suggest that hydrothermal fluids may have a Ni stable isotope composition of ~ 1.5 ‰. Thus hydrothermal sources may be contributing to the isotopic composition noted in the marine sediments herein.

~~———~~However, both marine sediments (this study) and ferromanganese crusts (Gall et al., 2013) are at least in part recording isotopic fractionation from a source that is isotopically heavier than riverine and hydrothermal Ni influxes. As continental weathering is a primary source of Ni to the global oceans, it is likely that weathering-induced isotope fractionation could account for the isotopically heavy Ni composition of organic-rich marine sediments. Further, the heavy Ni isotope signature observed in these sediments may reflect the contribution of heavy dissolved Ni to the oceans following retention of the lighter Ni isotopes during

weathering of oxyhydroxide phases (eg. Wasylenki et al., 2014).- In support of this, analysis of ferromanganese crusts at varying distances from the continental shelf (Gall et al., 2013) demonstrates that crusts growing in proximity to a continental shelf contain the heaviest Ni isotope compositions. However, although weathering does affect the isotopic composition of marine sediments, the effects resulting from additional factors such as riverine particulates , ~~Mn-oxides~~ and organic compounds have yet to be constrained (Cameron and Vance, 2014).

In addition, following examination of Ni isotope data from microorganisms (δ^{60}Ni = ~0.0 to -1.6 ‰; Cameron et al., 2009), it can be noted that the Ni isotope ratios in the organic-rich sediments herein (δ^{60}Ni = ~0.28 – 2.50 ‰) appear to have been driven in the opposite direction to those of the microorganisms. Whilst the causes of Ni isotope fractionation in these sediments are currently poorly understood, it appears that there is a fractionation effect associated with the Ni isotope system that may have parallels to the carbon isotope system, with the microorganisms taking up isotopically lighter Ni, thus potentially leaving behind an isotopically heavier Ni isotope signature in the sediment. Although it is impossible to draw a definitive conclusion from the current dataset, this study suggests that microorganisms and organic matter may play a key role in our understanding of Ni isotope fractionation (in a similar manner to the rhenium-osmium isotope system; Cumming et al., 2012; Harris et al., 2013) in organic-rich marine sediments, and as such, the importance of further investigation is emphasised.

7. Conclusions

This first investigation into the Ni stable isotope composition of organic-rich marine sediments from two distinct basins has yielded a number of key observations, outlined below.

1. This preliminary dataset indicates that organic-rich sediments have a Ni stable isotope composition (δ^{60}Ni) of 0.28 to 2.50 ‰.

2. No relationship is observed between the Ni stable isotope composition of the organic-rich sediments and TOC, suggesting that fractionation is not determined by changes in the organic carbon reservoir.

3. Similarly, there is no correlation between δ^{60}Ni and Ni abundance or bottom-water redox conditions, suggesting that the process of Ni uptake and enrichment at the sediment-water interface, and the degree of oxygenation in the water-column do not exert primary control on isotopic fractionation.

~~2~~4. The Ni isotope composition of marine sediments is substantially heavier and isotopically distinct to those of abiotic terrestrial and extraterrestrial samples (δ^{60}N values of -0.1 to 0.3 ‰; Cameron et al., 2009).

~~3~~5. Ni isotopes in marine sediments are isotopically heavier than those in present-day seawater and rivers (δ^{60}Ni = 1.44 ± 0.15 ‰ and 0.29 to 1.34~~0.8~~0 ‰, respectively;

Cameron and Vance, 2014)~~.~~, indicating input of an isotopically heavier source of Ni to the ocean.

~~4~~6. The observed range of δ^{60}N values in marine sediments is comparable to that of ferromanganese crusts (0.9 to 2.5 ‰; Gall et al., 2013). Adsorption of Ni to Fe-Mn oxyhydroxides results in the retention of isotopically light Ni and the mobilisation of isotopically heavier Ni during oxidative weathering (Wasylenki et al., 2014). Subsequently, the dissolved riverine load is enriched in heavier Ni. It is therefore probable that isotopic fractionation driven by the weathering environment plays a key role in yielding the range of δ^{60}N values that are observed in marine sediments.

~~5. No relationship is observed between the Ni stable isotope composition of the organic-rich sediments and TOC, suggesting that fractionation is not determined by changes in the organic carbon reservoir.~~

~~6. Similarly, there is no correlation between δ^{60}Ni and Ni abundance or bottom-water redox conditions, suggesting that the process of Ni uptake and enrichment at the sediment water interface, and the degree of oxygenation in the water column do not exert primary control on isotopic fractionation.~~

7. ~~Following evidence from Gall et al. (2013), it is probable the continental weathering process may induce isotopic fractionation.~~ The relatively heavy Ni stable isotope composition of marine sediments may also in part reflect influxes of dissolved Ni from hydrothermal sources (δ^{60}Ni = 1.5 ‰; Gall et al., 2013). However, further work is needed to investigate this.

The complexity of the sediment-seawater system may be the key factor that causes such enhanced levels of Ni isotope fractionation in marine sediments relative

582 to meteorites, basalts and continental sediments. This preliminary dataset has
583 produced some new and important data that can be the basis for further research of
584 Ni in organic-rich marine sediments. As such, it is recommended that the
585 relationships between Ni isotope fractionation and factors ubiquitous to the marine
586 depositional system, such as bottom-water redox conditions, the type of organic
587 matter present, organic matter preservation and TOC, are further explored.
588
589
590 **Figure captions**
591
592 Figure 1: Map and photograph showing the location of the Sinemurian-Pliensbachian
593 GSSP section, Robin Hood's Bay, UK.
594
595 Figure 2: Graphic log showing the Sinemurian-Pliensbachian boundary GSSP and the
596 relative locations of the samples analysed in this study. Samples used for Ni isotope
597 analysis are in bold. Bed number classification taken from Hesselbo and Jenkyns
598 (1995).
599
600 Figure 3: Present-day maturity map of the Exshaw Formation within Alberta, Canada
601 (modified from Creaney and Allan, 1991). Map shows the location of the thermally
602 immature, mature and overmature zones parallel to the Rocky Mountain Front, and
603 the location of the well from which the core samples used in this study originate.
604

Figure 4: Nickel isotope (δ^{60}Ni), Ni abundance, and TOC profiles for the Sinemurian-Pliensbachian section, presented against a corresponding stratigraphic column and graphic log. Black dashed line indicates the position of the Sinemurian-Pliensbachian boundary. [1]Bed numbers are from Hesselbo and Jenkyns (1995).

Figure 5: Plot showing the relationship between TOC and V/(V+Ni) for the Pennsylvanian Stark Shale Member samples (solid black squares) detailed in Hatch and Leventhal (1992), Robin Hood's Bay sediments (hollow diamonds ~~diamonds~~; this study) and the Exshaw Formation shales (hollow triangles; this study). Black dashed lines mark the parameters discussed in Hatch and Leventhal (1992), whereby values of > 2.5 wt. % TOC correspond to V/(V+Ni) values > 0.75 for the Pennsylvanian Stark Shale Member.

Figure 6: Nickel stable isotope data for organic-rich marine sediments from Robin Hood's Bay, UK (RHB) and the Exshaw Formation. The grey box represents the average of the Ni isotope data for meteorites, basalts and continental sediments (~0.2 ‰ and 1 standard deviation either side of this; Cameron et al., 2009). The white circles show Ni isotope data from ferromanganese crusts (taken from Gall et al., 2013).

Table 1: Previously established values for the trace element ratios and their corresponding depositional paleoredox conditions.

628 Table 2: Summary of trace element and TOC data and the associated ratios used for
629 paleoredox proxies, for the Robin Hood's Bay and Exshaw Formation marine
630 sediments.
631
632 Table 3: New nickel stable isotope data for a selection of Robin Hood's Bay and
633 Exshaw Formation marine sediments.
634
635 Table 4: A summary of elemental data for average shale, average upper continental
636 crust, Robin Hood's Bay and Exshaw Formation marine sediments.
637
638
639
640
641
642
643
644
645
646
647
648
649
650
651

652 **References**

653

654 Alberdi, M., and Lafargue, E., 1993, Vertical variations of organic matter content in
655 Guayuta Group (upper Cretaceous), Interior Mountain Belt, Eastern
656 Venezuela: Organic Geochemistry, v. 20, no. 4, p. 425-436.

657 Birck, J. L., and Lugmair, G. W., 1988, Nickel and chromium isotopes in Allende
658 inclusions: Earth and Planetary Science Letters, v. 90, no. 2, p. 131-143.

659 Brennecka, G. A., Wasylenki, L. E., Bargar, J. R., Weyer, S., and Anbar, A. D., 2011,
660 Uranium Isotope Fractionation during Adsorption to Mn-Oxyhydroxides:
661 Environmental Science and Technology, v. 45, no. 4, p. 1370-1375.

662 Cameron, V., Vance, D., Archer, C., and House, C. H., 2007, Nickel stable isotopes as
663 biogeochemical tracers, Goldschmidt Conference Abstracts, p. A141.

664 Cameron, V., Vance, D., Archer, C., and House, C. H., 2009, A biomarker based on the
665 stable isotopes of nickel: Proceedings of the National Academy of Sciences, v.
666 106, p. 10944-10948.

667 Cameron, V., Vance, D., and Poulton, S., 2011, Nickel isotopes, BIFs and the Archean
668 oceans, Goldschmidt Conference Abstracts, Mineralogical Magazine, p. 615.

669 Cameron, V., House, C. H., and Brantley, S. L., 2012, A First Analysis of Metallome
670 Biosignatures of Hyperthermophilic Archea: Archea, v. 2012, p. 1-12.

671 Cameron, V., and Vance, D., 2014, Heavy nickel isotope compositions in rivers and
672 the oceans, Geochimica et Cosmochimica Acta, v. 128, p. 195-211.

673 Caplan, M. L., and Bustin, R. M., 1998, Sedimentology and sequence stratigraphy of
674 Devonian-Carboniferous strata, southern Alberta: Bulletin of Canadian
675 Petroleum Geology, v. 46, p. 487-514.

676 Caplan, M. L., and Bustin, R. M., 1999, Palaeoceanographic controls on geochemical
677 characteristics of organic-rich Exshaw mudrocks: role of enhanced primary
678 production: Organic Geochemistry, v. 30, no. 2-3, p. 161-188.
679 Chen, J. H., Papanastassiou, D. A., and Wasserburg, G. J., 2009, A search for nickel
680 isotopic anomalies in iron meteorites and chondrites: Geochimica et
681 Cosmochimica Acta, v. 73, no. 5, p. 1461-1471.
682 Cook, D. L., Wadhwa, M., Clayton, R., Dauphas, N., Janney, P. E., and Davis, A. M.,
683 2007, Mass-dependent fractionation of nickel isotopes in meteoritic metal:
684 Meteoritics and Planetary Science, v. 42, no. 12, p. 2067-2077.
685 Creaney, S., and Allan, J., 1991, Hydrocarbon generation and migration in the
686 Western Canada sedimentary basin: Geological Society, London, Special
687 Publications, v. 50, no. 1, p. 189-202.
688 Creaser, R. A., Sannigrahi, P., Chacko, T., and Selby, D., 2002, Further evaluation of
689 the Re-Os geochronometer in organic-rich sedimentary rocks: a test of
690 hydrocarbon maturation effects in the Exshaw Formation, Western Canada
691 Sedimentary Basin: Geochimica et Cosmochimica Acta, v. 66, no. 19, p. 3441-
692 3452.
693 Cumming, V. M., Selby, D., and Lillis, P., 2012, Re-Os geochronology of the lacustrine
694 Green River Formation: Insights into direct depositional dating of lacustrine
695 successions, Re-Os systematics and paleocontinental weathering: Earth and
696 Planetary Science Letters, v. 359-360, p. 194-205.
697 Dean, W. T., Donovan, D. T., and Howarth, M. K., 1961, The Liassic ammonite Zones
698 and Subzones of the North West European Province: Bulletin of the Natural
699 History Museum, v. 4, p. 435-505.

Dera, G., Pucéat, E., Pellenard, P., Neige, P., Delsate, D., Joachimski, M. M., Reisberg, L., and Martinez, M., 2009, Water mass exchange and variations in seawater temperature in the NW Tethys during the Early Jurassic: Evidence from neodymium and oxygen isotopes of fish teeth and belemnites: Earth and Planetary Science Letters, v. 286, no. 1-2, p. 198-207.

Dewaker, K. N., Chandra, K., Arunachalam, J., and Karunasagar, D., 2000, Isotopic fractionation of Ni60/Ni61 in kerogen and bitumen samples: Current Science, v. 79, no. 12, p. 1720-1723.

Dill, H., 1986, Metallogenesis of early Paleozoic graptolite shales from the Graefenthal Horst (Northern Bavaria-Federal Republic of Germany): Economic Geology, v. 81, p. 889-903.

Ellrich, J., Hirner, A., and Stärk, H., 1985, Distribution of trace elements in crude oils from southern Germany: Chemical Geology, v. 48, no. 1-4, p. 313-323.

Frausto da Silva, J.J.R., and Williams, R.J.P., 2001, The Biological Chemistry of the Elements: The Inorganic Chemistry of Life, Oxford University Press, Oxford, p. 436-449.

Gall, L., Williams, H., Siebert, C., and Halliday, A., 2012, Determination of mass-dependent variations in nickel isotope compositions using double spiking and MC-ICPMS: Journal of Analytical Atomic Spectrometry, v. 27, no. 1, p. 137-145.

Gall, L., Williams, H. W., Siebert, C., Halliday, A. N., Herrington, R. J., and Hein, J. R., 2013, Nickel isotopic compositions of ferromanganese crusts and the constancy of deep ocean inputs and continental weathering effects over the Cenozoic: Earth and Planetary Science Letters, v. 375, p. 148-155.

724 Gradstein, F. M., Ogg, J. G., Schmitz, M .D., and Ogg, G. M. 2012. The Geologic Time
725 Scale 2012. Elsevier.
726 Harris, N. B., Mnich, C. A., Selby, D., and Korn, D., 2013, Minor and trace element and
727 Re-Os chemistry of the Upper Devonian Woodford Shale, Permian Basin,
728 west Texas: Insights into metal abundance and basin processes: Chemical
729 Geology, v. 356, p. 76-93.
730 Hatch, J. R., and Leventhal, J. S., 1992, Relationship between inferred redox potential
731 of the depositional environment and geochemistry of the Upper
732 Pennsylvanian (Missourian) Stark Shale Member of the Dennis Limestone,
733 Wabaunsee County, Kansas, U.S.A: Chemical Geology, v. 99, no. 1-3, p. 65-82.
734 Herzog, G. F., hall, G. S., and Brownlee, D. E., 1994, Mass fractionation of nickel
735 isotopes in metallic cosmic spheres: Geochimica et Cosmochimica Acta, v. 58,
736 no. 23, p. 5319-5323.
737 Hesselbo, S. P., and Jenkyns, H. C., 1995, A comparison of the Hettangian to Bajocian
738 successions of Dorset and Yorkshire, *in* Taylor, P. D., ed., Field Geology of the
739 British Jurassic, Geological Society, London, p. 105-150.
740 Hesselbo, S. P., Meister, C., and Grocke, D. R., 2000, A potential global stratotype for
741 the Sinemurian-Pliensbachian boundary (Lower Jurassic), Robin Hood's Bay,
742 UK: ammonite faunas and isotope stratigraphy: Geological Magazine, v. 137,
743 no. 6, p. 601-607.
744 Jones, B., and Manning, D. A. C., 1994, Comparison of geochemical indices used for
745 the interpretation of palaeoredox conditions in ancient mudstones: Chemical
746 Geology, v. 111, no. 1-4, p. 111-129.

747 Jones, C. E., Jenkyns, H. C., and Hesselbo, S. P., 1994, Strontium isotopes in Early
748 Jurassic seawater: Geochimica et Cosmochimica Acta, v. 58, no. 4, p. 1285-
749 1301.
750 Kohman, T. P., and Robison, M. S., 1980, Iron-60 as a possible heat source and
751 chronometer in the early solar system: Lunar and Planetary Science, v. 11, p.
752 564-566.
753 Konhauser, K. O., Pecoits, E., Lalonde, S. V., Papineau, D., Nisbet, E. G., Barley, M. E.,
754 Arndt, N. T., Zahnle, K., and Kamber, B. S., 2009, Oceanic nickel depletion and
755 a methanogen famine before the Great Oxidation Event: Nature, v. 458, p.
756 750-753.
757 Leenheer, M. J., 1984, Mississippian Bakken and other equivalent formations as
758 source rocks in the Western Canada basin: Organic Geochemistry, v. 6, p.
759 521-533.
760 Lewan, M. D., 1984, Factors controlling the proportionality of vanadium to nickel in
761 crude oils: Geochimica et Cosmochimica Acta, v. 48, no. 11, p. 2231-2238.
762 Lewan, M. D., and Maynard, J. B., 1982, Factors controlling enrichment of vanadium
763 and nickel in the bitumen of organic sedimentary rocks: Geochimica et
764 Cosmochimica Acta, v. 46, no. 12, p. 2547-2560.
765 Li, H.-Y., Schoonmaker, J., 2003, Chemical composition and mineralogy of marine
766 sediments. In: Treatise on Geochemistry. Sediments, Diagenesis, and
767 Sedimentary Rocks, v. 7, p. 1-35.
768 López, L., Lo Mónaco, S., Galarraga, F., Lira, A., and Cruz, C., 1995, VNi ratio in
769 maltene and asphaltene fractions of crude oils from the west Venezuelan
770 basin: correlation studies: Chemical Geology, v. 119, no. 1-4, p. 255-262.

771 Manning, L. K., Frost, C. D., and Branthaver, J. F., 1991, A neodymium isotopic study
772 of crude oils and source rocks: potential applications for petroleum
773 exploration: Chemical Geology, v. 91, no. 2, p. 125-138.
774 Meijer, N. C., Johnston, D. I., and Fullmer, E. G., 1994, Devonian stratigraphy and
775 depositional history across Peace River Highland, west central Alberta and
776 nearby British Columbia: Geological Survey of Canada Open File 2851, p. 40
777 pp.
778 Meister, C., Aberhan, M., Blau, J., Dommergues, J.-L., Feist-Burkhardt, S., Hailwood,
779 E. A., Hart, M., Hesselbo, S. P., Hounslow, M. W., Hylton, M., Morton, N.,
780 Page, K., and Price, G. D., 2006, The Global Boundary Stratotype Section and
781 Point (GSSP) for the base of the Pliensbachian Stage (Lower Jurassic), Wine
782 Haven, Yorkshire, UK: Episodes, v. 29, no. 2, p. 93-114.
783 Morand, P., and Allègre, C. J., 1983, Nickel isotopic studies in meteorites: Earth and
784 Planetary Science Letters, v. 63, no. 2, p. 167-176.
785 Moynier, F., Blichert-Toft, J., Telouk, P., Luck, J.-M., and Albarède, F., 2007,
786 Comparative stable isotope geochemistry of Ni, Cu, Zn, and Fe in chondrites
787 and iron meteorites: Geochimica et Cosmochimica Acta, v. 71, no. 17, p.
788 4365-4379.
789 Ottley, C. J., Pearson, D. G., and Irvine, G. J., 2003, A routine method for the
790 dissolution of geological samples for the analysis of REE and trace elements
791 via ICP-MS, *in* Holland, G., and Tanner, S. D., eds., Plasma source mass
792 spectrometry: applications and emerging technologies, p. 221-230.

793 Palmer, M. R., Kenison Falkner, K., Turekian, K. K., and Calvert, S. E., 1988, Sources of
794 osmium isotopes in manganese nodules: Geochimica et Cosmochimica Acta,
795 v. 52, no. 5, p. 1197-1202.
796 Peucker-Ehrenbrink, B., and Hannigan, R. E., 2000, Effects of black shale weathering
797 on the mobility of rhenium and platinum group elements: Geology, v. 28, no.
798 5, p. 475-478.
799 Piggott, N., and Lines, M. D., 1992, A case study of migration from the West Canada
800 Basin, *in* England, W. A., and Fleet, A. J., eds., Petroleum Migration, Volume
801 59, Geological Society Special Publication, p. 207-225.
802 Powell, J. H., 1984, Lithostratigraphical nomenclature of the Lias Group in the
803 Yorkshire Basin: Proceedings of the Yorkshire Geological Society, v. 45, p. 51-
804 57.
805 Quitté, G., Meier, M., Latkoczy, C., Halliday, A.N., and Günther, D., 2006, Nickel
806 isotopes in iron meteorites–nucleosynthetic anomalies in sulphides with no
807 effects in metals and no trace of ^{60}Fe: Earth and Planetary Science Letters, v.
808 242, p. 16-25.
809 Quitté, G., and Oberli, F., 2006, Quantitative extraction and high precision isotope
810 measurements of nickel by MC-ICPMS: Journal of Analytical Atomic
811 Spectrometry, v. 21, p. 1249-1255.
812 Richards, B. C., and Higgins, A. C., 1988, Devonian-Carboniferous beds of the Palliser
813 and Exshaw formations at Jura Creekm Rocky Mountains, southwestern
814 Alberta, *in* McMillan, N. J., ed., Devonian of the world, Canadian Society of
815 Petroleum Geologists Memoir, Volume 14, p. 399-412.

816 Richards, B. C., Mamet, B. L., and Bamber, E. W., 1999, Uppermost Devonian and
817 Carboniferous sequence stratigraphy, biostratigraphy and basin
818 development, Banff region, southwestern Alberta, XIV International Congress
819 on the Carboniferous and Permian, Field Trip, 4-7 and 4-17 Guidebook:
820 Calgary, Alberta.
821 Richards, C., Ross, G. M., and Utting, J., 2002, U-Pb geochronology, lithostratigraphy
822 and biostratigraphy of tuff in the Upper Famennian to Tournaisian Exshaw
823 Formation: Evidence for a mid-Paleozoic magmatic arc on the northwestern
824 margin of North America, *in* Hills, L. V., Henderson, C. M., and Bamber, E. W.,
825 eds., Carboniferous and Permian of the World: XIV ICCP Proceedings, Volume
826 19, Can Soc Petrol Geol Mem, p. 158-207.
827 Rimmer, S. M., 2004, Geochemical paleoredox indicators in Devonian-Mississippian
828 black shales, Central Appalachian Basin (USA), Chemical Geology, v. 206, no.
829 3-4, p. 373-391.
830 Rudnick, R. L., and Gao, S., 2003, 3.01 Composition of the Continental Crust: Treatise
831 on Geochemistry, v. 3, p. 1-64.
832 Schovsbo, N. H., 2001, Why barren intervals? A taphonomic case study of the
833 Scandinavian Alum Shale and its faunas: Lethaia, v. 34, no. 4, p. 271-285.
834 Sclater, F., Boyle, E., Edmond, J., 1976, On the marine geochemistry of nickel: Earth
835 and Planetary Science Letters, v. 31, p. 119-128.
836 Selby, D., and Creaser, R. A., 2005, Direct radiometric dating of the Devonian-
837 Mississippian time-scale boundary using the Re-Os black shale
838 geochronometer: Geology, v. 33, p. 545-548.

839 Selby, D., Mutterlose, J., and Condon, D. J., 2009, U-Pb and Re-Os geochronology of
840 the Aptian/Albian and Cenomanian/Turonian stage boundaries: Implications
841 for timescale calibration, osmium isotope seawater composition and Re-Os
842 systematics in organic-rich sediments: Chemical Geology, v. 265, no. 3-4, p.
843 394-409.
844 Sellwood, B. W., and Jenkyns, H. C., 1975, Basins and swells and the evolution of an
845 epeiric sea (Pliensbachian-Bajocian of Great Britain): Journal of the Geological
846 Society, v. 131, no. 4, p. 373-388.
847 Shimamura, T., and Lugmair, G. W., 1983, Ni isotopic compositions in Allende and
848 other meteorites: Earth and Planetary Science Letters, v. 63, no. 2, p. 177-
849 188.
850 Spath, L. F., 1923, Correlation of the Ibex and Jamesoni Zones of the Lower Lias:
851 Geological Magazine, v. 60, p. 6-11.
852 Wasylenki, L., Spivak-Birndorf, L., Howe, H., and Wells, R., 2014, Experiments reveal
853 the mechanism by which Ni isotopes fractionate in the weathering
854 environment: Goldschmidt Abstracts, 2661.
855 Wasylenki, L. E., Rolfe, B. A., Weeks, C. L., Spiro, T. G., and Anbar, A. D., 2008,
856 Experimental investigation of the effects of temperature and ionic strength
857 on Mo isotope fractionation during adsorption to manganese oxides:
858 Geochimica et Cosmochimica Acta, v. 72, p. 5997-6005.
859 Wasylenki, L. E., Weeks, C. L., Bargar, J. R., Spiro, T. G., Hein, J. R., and Anbar, A. D.,
860 2011, The molecular mechanism of Mo isotope fractionation during
861 adsorption to birnessite: Geochimica et Cosmochimica Acta, v. 75, no. 17, p.
862 5019-5031.

Wedepohl, K. H., 1971, Environmental influences on the chemical composition of shales and clays: Physics and Chemistry of the Earth, v. 8, p. 305-333.

Xue, S., Herzog, G. F., Hall, G. S., Klein, J., Middleton, R., and Juenemann, D., 1995, Stable nickel isotopes and cosmogenic beryllium-10 and aluminum-26 in metallic spheroids from Meteor Crater, Arizona: Meteoritics, v. 30, p. 303-310.

Characterising the nickel isotopic composition of organic-rich marine sediments

Highlights

- New Ni stable isotope data for two suites of organic-rich marine sediments (ORMS)
- The Ni isotope compositions (Ni IC) of both suites are comparable
- The Ni IC of ORMS are heavier than bulk Earth samples and present-day seawater
- The Ni IC of ORMS are comparable to that of ferromanganese crusts
- Factors ubiquitous to the marine realm are likely to drive fractionation in ORMS

Characterising the nickel isotopic composition of organic-rich marine sediments

Sarah J. Porter[1,2*], David Selby[1], and Vyllinniskii Cameron[3]

[1] Department of Earth Sciences, Science Labs, Durham University, Durham, DH1 3LE, UK
[2] Chemostrat Ltd., Unit 1 Ravenscroft Court, Buttington Cross Enterprise Park, Welshpool, Powys, SY21 8SL, UK
[3] Bristol Isotope Group, School of Earth Sciences, University of Bristol, Bristol BS8 1RJ, UK

[*]Corresponding author: Sarah J. Porter. Email: sarahporter@chemostrat.com; Tel.:+44(7889)838599

Keywords: Nickel isotope fractionation, Ni isotopes, δ^{60}Ni, organic-rich marine sediments, Sinemurian-Pliensbachian GSSP, Exshaw Formation, redox

Abstract

New Ni stable isotope data (δ^{60}Ni) determined by double-spike MC-ICP-MS for two geologically distinct suites of organic-rich marine sediments from the Sinemurian-Pliensbachian (S-P) Global Stratotype Section and Point (GSSP; Robin Hood's Bay, UK) and the Devonian-Mississippian Exshaw Formation (West Canada Sedimentary Basin) is presented herein. These sediments yield δ^{60}Ni values of between 0.2 ‰ and 2.5 ‰, and predominantly have Ni isotopic compositions that are heavier than those of abiotic terrestrial and extraterrestrial samples (0.15 ‰ and 0.27 ‰), and in some cases present-day seawater (1.44 ‰) and dissolved Ni from riverine input (0.80 ‰). In addition, the observed degree of isotopic fractionation in the marine sediments is far greater than that of these other sample matrices. However, a strong similarity is exhibited between the δ^{60}Ni values of the organic-rich sediments studied here and those of ferromanganese crusts (0.9 to 2.5 ‰), suggesting that factors ubiquitous to

33 the marine environment are likely to play a key role in the heightened level of
34 isotopic fractionation in these sample matrices.
35 A lack of correlation between the Ni stable isotope compositions of the organic-rich
36 sediments and Ni abundance, suggests that isotopic fractionation in these sediments
37 is not controlled by incorporation or enrichment of Ni during sediment
38 accumulation. Further, no relationship is observed between δ^{60}Ni and TOC
39 concentrations or bottom-water redox conditions, indicating that the organic carbon
40 reservoir and levels of oxygenation at the sediment-water interface do not exert a
41 primary control on Ni isotope fractionation in marine sediments. Following
42 examination of these relationships, it is therefore more likely that the heavy Ni
43 isotope compositions of marine sediments are controlled by the weathering
44 environment and the dominant sources of dissolved Ni into the global ocean
45 reservoir.
46
47
48
49
50
51
52
53
54
55
56

57

58 **1. Introduction**

59

60 For several decades previous investigations of Ni isotopes have focused
61 predominantly on characterising radiogenic isotopic fractionation in extraterrestrial
62 materials, with a view to enhancing our understanding of planetary processes and
63 the isotopic composition of the early Solar System (eg. Kohman and Robison, 1980;
64 Morand and Allègre, 1983; Shimamura and Lugmair, 1983; Birck and Lugmair, 1988;
65 Herzog et al*.,* 1994; Xue et al*.,* 1995; Quitté et al*.,* 2006; Cook et al*.,* 2007; Moynier et
66 al*.,* 2007; Chen et al*.,* 2009). Further, the role of Ni as a bioessential trace metal (eg.
67 Frausto da Silva and Williams, 2001; Cameron et al*.,* 2007; 2009) has led to the
68 recognition that the stable isotopes of Ni may have the potential to be utilised as a
69 powerful biological tool for studies of early life on Earth (Cameron et al*.,* 2009;
70 2012).

71 In addition to its role in cosmochemical and biochemical investigations, the
72 potential of Ni to significantly enhance our understanding of organic-rich
73 sedimentary environments and to provide a powerful geological tracer in the
74 petroleum realm has been recognised, following pioneering work by Lewan and
75 Maynard (1982) and Lewan (1984) (eg. Ellrich et al*.,* 1985; Manning et al*.,* 1991;
76 Alberdi and Lafargue, 1993; López et al*.,* 1995). However, these studies focused on
77 the elemental distribution of Ni rather than on its isotopic characterisation, and as
78 such, no study currently exists that evaluates the behaviour of Ni stable isotopes in
79 organic-rich sediments or indeed within a stratigraphic profile. This can be attributed
80 to Ni being a relatively newly investigated system, together with the difficulty

81 associated with purifying Ni from such complex sample matrices, that has only
82 recently been overcome through advancements in analytical and mass spectrometry
83 techniques (eg. Gall et al., 2012; Cameron and Vance, 2014).

84 Until now, Ni stable isotope systematics in organic-rich sedimentary matrices
85 have not been investigated. Indeed, it is only recently that the Ni isotopic
86 composition of seawater and the sources of Ni to the global oceanic reservoir have
87 been determined (e.g. Cameron and Vance, 2014; Gall et al., 2013). Present-day
88 seawater has an average δ^{60}Ni value of 1.44 ± 0.15 ‰, with apparent global isotopic
89 homogeneity (Cameron and Vance, 2014). The oceanic residence time of Ni has been
90 calculated as ~30 kyr (Cameron and Vance, 2014), which is significantly longer than
91 the mixing time of the global oceans (~2,000 yrs; Palmer et al., 1988). This would be
92 sufficient for the ocean to have an isotopically homogenous Ni composition.
93 Cameron et al. (2014) also demonstrate that draw-down of Ni from the surface to
94 deep ocean during trace metal cycling is not accompanied by isotopic fractionation,
95 thus further suggesting that the modern ocean is isotopically homogenous. In the
96 absence of any Ni isotope studies on banded iron formation and shale datasets, it is
97 difficult to speculate on processes occurring in an ancient ocean. However,
98 examination of Ni/Fe data from banded iron formations and extrapolated maximum
99 dissolved Ni concentration values in sea water through time (Konhauser et al., 2009),
100 demonstrates that dissolved nickel concentrations may have reached present day
101 values by ~550 Ma. As such, given the age of the sediments being studied herein
102 (~190-360 Ma), it is appropriate to use what we know regarding modern ocean
103 circulation and fractionation processes to hypothesise about processes acting in the
104 ancient oceans. The predominant input of dissolved Ni to the oceans occurs via

105 riverine influx, which has been suggested to yield an annual discharge- and
106 concentration-weighted δ^{60}Ni average of +0.80 ‰ (Cameron and Vance, 2014).
107 Significant variability in the riverine isotopic composition has been observed (+0.29
108 to +1.34 ‰), which has been attributed to isotopic fractionation of Ni during
109 weathering of continental crust, resulting in heavier δ^{60}Ni values in rivers and
110 seawater. In addition, mineral dust and volcanic ash also contribute to the oceanic Ni
111 budget (Li and Schoonmaker, 2003), as well as hydrothermal vent fluids (δ^{60}Ni = 1.5
112 ‰; Gall et al., 2012).

113 Herein we present the first attempt at creating a Ni isotope stratigraphic
114 profile for an organic-rich sedimentary succession. The marine section across the
115 Sinemurian-Pliensbachian Global Stratotype Section and Point (GSSP), Robin Hood's
116 Bay, UK, is ideally suited to the present study, as it well understood
117 biostratigraphically (Hesselbo et al., 2000; Meister et al., 2006) and has been
118 previously characterised using other isotope stratigraphy techniques, including
119 strontium (^{87}Sr/^{86}Sr; Jones et al., 1994; Hesselbo et al., 2000), oxygen (δ^{18}O), carbon
120 (δ^{13}C) (Hesselbo et al., 2000), and Re-Os isotopes (Porter et al., 2013). The section is
121 also consistently thermally immature (the rocks have not been subjected to enough
122 heat or pressure to convert any kerogens present to hydrocarbons), thereby
123 eliminating any potential effects of thermal maturation on the Ni isotope signature.
124 In addition, to draw comparison between the isotopic composition of samples of
125 different depositional ages and environments, we present Ni isotope data from a
126 selection of thermally immature black shale samples from a core of the Exshaw
127 Formation, Canada.

128 To accurately assess and interpret any stratigraphic variation of Ni isotopes in
129 the Robin Hood's Bay section and Exshaw Formation samples, it is critical to
130 determine whether any fluctuations in paleoredox conditions occur. Nickel primarily
131 occupies one oxidation state in the natural environment (Ni^{2+}), suggesting that it is
132 not redox sensitive. However, its preferential association with redox-sensitive
133 metallo-organic complexes (porphyrins) in organic-rich sediments (Lewan and
134 Maynard, 1982) indicates that certainly within these sample matrices, redox
135 conditions at the time of sediment deposition may directly impact the degree of
136 enrichment or depletion of Ni. Herein, paleoredox conditions have been established
137 for the Sinemurian-Pliensbachian GSSP section and the Exshaw Formation sample
138 suite. Although one previous study (Dewaker et al., 2000) provides a preliminary
139 dataset for the Ni isotope composition of sediments from 3 different basins, our
140 understanding of the behaviour of Ni isotope systematics within organic-rich
141 sediments is currently non-existent. Further, advancements in analytical techniques
142 over the past decade suggest that the methodology employed by Dewaker et al.
143 (2000) may not have been optimal for Ni separation or Ni stable isotope analysis.
144 This paper presents the first detailed study of nickel stable isotope
145 systematics in organic-rich marine sediments. Analysis of marine sediments of
146 different depositional ages and from two geologically distinct settings, the
147 Sinemurian-Pliensbachian boundary (UK) and the Devonian-Mississippian Exshaw
148 Formation (Canada), yields comparable Ni isotope compositional values for both
149 sites. These samples provide insight into the incorporation of Ni into ocean
150 sediments, and allow evaluation of the contribution of the various dissolved Ni fluxes
151 to the seawater during these time periods.

2. Geological Setting

2.1 The Sinemurian-Pliensbachian boundary GSSP, Robin Hood's Bay, UK

The Sinemurian-Pliensbachian boundary, established from the succession's complete ammonite assemblages (Spath, 1923; Dean et al*.,* 1961; Hesselbo et al*.,* 2000; Meister et al*.,* 2006), occurs in the Pyritous Shales of the Redcar Mudstone Formation within the Lias Group at Robin Hood's Bay (Powell, 1984; Fig. 1). At this point in the Early Jurassic, Robin Hood's Bay was positioned on the margins of a shallow epicontinental sea (eg. Dera et al*.,* 2009) that covered most of Northern Europe, including Britain, during the Mesozoic (Sellwood and Jenkyns, 1975). The facies changes across the boundary, from pale siliceous to finer, more organic-rich mudstones (Fig. 2), indicate an overall relative increase in sea level of at least regional extent (eg. Hesselbo et al*.,* 2000; Meister et al*.,* 2006; Porter et al., 2013).

The age for the base of the Pliensbachian has been defined by the Geological Time Scale (GTS) 2012 as 189.6 ± 1.5 Ma (Gradstein et al., 2012), derived from cycle-scaled linear Sr trends and ammonite occurrences (as noted above; also includes the lowest occurrence of *Bifericeras donovani*; Gradstein et al., 2012).

2.2 Exshaw Formation, West Canada Sedimentary Basin (WCSB)

The West Canada Sedimentary Basin (WCSB) trends approximately NW-SE between the Canadian Shield to the East and the Western Cordillera to the West

(Piggott and Lines, 1992). Within the WCSB lies the Exshaw Formation, a thin but laterally continuous unit (2-12 m thick; Leenheer, 1984; Creaney and Allan, 1991). The Exshaw Formation in south-west and western Alberta (Fig. 3) comprises a lower member of organic-rich mudrocks and black shales which rest with minor disconformity upon Upper Devonian carbonate strata (Richards et al*.,* 1999), and are abruptly to gradationally overlain by bioturbated shelf siltstones (Caplan and Bustin, 1998, 1999; Creaser et al*.,* 2002). The depositional interval of the lower black shale unit is well constrained biostratigraphically; between the *expansa* and *duplicata* zones of Late Famennian to Early Tournaisian time (over a maximum time period of ~363 – 360 Ma; Caplan and Bustin, 1998). These lower black shales are dark grey, bituminous, relatively thin (consistently between 3-5 m; Meijer et al*.,* 1994) and widespread (Meijer et al*.,* 1994). The Devonian-Mississippian boundary (Exshaw-type section at Jura Creek, ~80 km west of Calgary, Alberta, Canada) represents the boundary between the upper calcareous and lower non-calcareous black shale units (Richards and Higgins, 1988). Selby and Creaser (2005) provide an absolute Model 1 Re-Os age for this boundary, and thus the top of the lower black shale unit, of 361.3 ± 2.4 Ma. In addition, U-Pb monazite data from a tuff horizon close to the base of the lower black shale member constrains an absolute depositional age for this unit of 363.4 ± 0.4 Ma (Richards et al*.,* 2002). Deposition at this time represents part of a continent-wide Famennian-Tournaisian black shale event, and in turn, a possible ocean anoxic event (Piggott and Lines, 1992).

3. Sampling

A set of 32 samples (SP7-09 to SP39-09) was collected from the Pyritous Shales Member of the Redcar Mudstone Formation, along a 6 m vertical section bracketing the Sinemurian–Pliensbachian boundary (sample SP22-09) at Robin Hood's Bay (Fig. 2). This marine sequence contains a rich fauna of ammonites both above and below the boundary interval (Hesselbo et al., 2000). Total organic carbon analysis was conducted on all samples, with a consistent sampling interval of ~20 cm for 3 m above and 3 m below the boundary from Beds 69–75 (except within Bed 72, where a smaller sampling interval of ~15 cm was used). Of these samples, 14 were analysed for Ni isotopes at a sampling interval of ~40 cm (Fig. 2).

Four samples from the Lower member of the Exshaw Formation were collected from the Alberta Energy and Utilities Board, Core Research Centre, Calgary (Fig. 3). The samples were taken from core 3-19-80-23W5, as detailed in Piggot and Lines (1992) and Creaser et al. (2002). All samples are thermally immature, fine-grained black shales containing very thin parallel and undulating laminations, and showing no evidence of post-depositional disturbance. Drill core samples were obtained to avoid any potential effects of surface weathering, including loss of organic matter (PeuckerEhrenbrink and Hannigan, 2000). Further, edges of the core were polished and where possible samples were taken from the central part of the core.

4. Analytical Protocol

4.1 Trace element abundance and TOC

The elements V, Cr, Ni and Co were analysed in this study in order to look at relative changes of depositional redox conditions in the sediments of interest. Samples were prepared for trace element analysis at the Durham Geochemistry Group (University of Durham, UK) following the method of Ottley et al*.,* (2003). Sample powders (~100 mg) were digested in a 4:1 solution of 29 N HF and 16 N HNO_3 at ~150 ^{o}C for 48 hrs. Samples were then evaporated to near rather than total dryness, to avoid stabilisation of insoluble fluorides (Ottley et al*.,* 2003). This was followed by the addition of 1 ml 16 N HNO_3 and evaporation to near dryness. The previous stage was repeated before the addition of 2.5 ml 16 N HNO_3 and ~10 ml 18MΩ water to create a ~4 N HNO_3 solution. Sample beakers were capped and heated on the hotplate overnight at ~100 ^{o}C. Once cooled, 1 ml of 1 ppm internal Re and Rh spike was added to the samples (to yield 20 ppb Re and Rh in the final analyte solution) before dilution up to 50 ml with MQ, yielding a ~0.5 N HNO_3 solution. Prior to analysis, samples were diluted 10-fold by taking 1 ml from the 50 ml solution and diluting it to 10 ml using 0.5 N HNO_3. Samples were then analysed using the Thermo X-Series Quadrupole Inductively Coupled Plasma Mass Spectrometer (ICP-MS).Replicate analyses of USGS International Reference Materials (RMs) AGV-1, BHVO-1 and W-2 were conducted for calibration per sample set.

Total organic carbon measurements were performed at Durham University using a Costech Elemental Analyser (ECS 4010) coupled to a ThermoFinnigan Delta V Advantage. Total organic carbon was obtained as part of the isotopic analysis ($\delta^{13}C_{org}$) using an internal standard (Glutamic Acid, 40.82 % C). Data accuracy was monitored through routine analyses of in-house standards, which are stringently

248 calibrated against international standards (eg. USGS 40, USGS 24, IAEA 600, IAEA
249 CH6).
250
251 *4.2 Nickel stable isotopes*
252 All Ni isotope analyses were conducted at the University of Bristol. Samples
253 (~100 mg) were digested in closed PFA Beakers (Savillex, Minnetonka, MN) in a
254 mixture of concentrated HF and HNO_3 (3:1) at 140 ^{o}C for 48 hrs. Dried samples were
255 treated further with 7 N HCl. Chemical separation, purification and analyses of Ni
256 isotopes was carried out as described in detail in Cameron et al. (2009) and Cameron
257 and Vance (2014). Briefly, sample aliquots were spiked and allowed to equilibrate
258 under heating in closed vials overnight. This was followed by drying down and
259 treatment with 7 N HCl + H_2O_2. The spiked samples were then put through a 3-stage
260 column procedure that in turn removes Fe and Zn, separates Ni from the bulk
261 sample matrix, and final purification to remove any residual Fe and Zn. The first ion-
262 exchange column (AG MP-1M, Bio-Rad) is used to remove Fe and Zn. The dried
263 samples are then taken up in 1M HCl/1 M ammonium citrate, and the pH adjusted to
264 8–9 before loading onto columns filled with Ni resin (Eichrom Technologies). This
265 step separates Ni while removing all other matrix elements in the sample. After
266 oxidation to remove Ni-bound DMG, the samples are finally put through a third
267 column, which is a repeat of the first anion column, to clean up any residual Fe and
268 Zn.
269 All analyses were conducted in low resolution mode using a ThermoFinnigan
270 Neptune multi-collector (MC) ICP-MS coupled to an Aridus desolvating nebuliser
271 system (CETAC, Omaha, NE, USA). Samples were introduced in 2% HNO_3 via a CPI

PFA nebuliser (50 μl/minute) and spray chamber. Prior to isotopic analysis, the $^{56}Fe/^{58}Ni$ ratio was manually checked in high resolution mode in all samples so that any potential isobaric interference from residual sample ^{58}Fe could be applied as a correction to Ni mass 58. Relative to the propagated internal uncertainty on $\delta^{60}Ni$, the correction was insignificant. Additionally, a small amount of N_2 was introduced to the Aridus sweep gas to reduce a potential interference from $^{40}Ar^{18}O$ at mass 58. To mitigate inaccuracies in the $\delta^{60}Ni$ brought on by any instrumental variations, measurements of the pure NIST SRM986 standard were made throughout the analytical session. The reproducibility and accuracy of all isotope ratios were monitored further by measurement of mixtures of the SRM986 standard with the double-spike. All isotopes were measured simultaneously in static mode using a multiple Faraday collector array. All Ni data are reported relative to NIST SRM986, in the standard delta notation ($\delta^{60}Ni = [(^{60}Ni/^{58}Ni)_{sample}/(^{60}Ni/^{58}Ni)_{NISTSRM986})-1] \times 1000$), with all uncertainties reported to the 2σ level.

5. Results

5.1 Trace elements and TOC

The trace element ratios Ni/Co, V/Cr and V/(V+Ni) have been utilised by previous studies to evaluate paleoredox conditions at the time of sediment deposition (eg. Hatch and Leventhal, 1992; Jones and Manning, 1994; Schovsbo, 2001; Rimmer, 2004). Both Ni and V occur in highly stable tetrapyrrole complexes that are originally derived from chlorophyll and are preferentially preserved under anoxic conditions (Lewan and Maynard, 1982). When organic matter has been

296 extensively exposed to aerobic conditions, preservation of these tetrapyrrole
297 complexes will be low and subsequently the organic matter will have low Ni and V
298 contents. Chromium is not influenced by redox conditions, and thus because of its
299 association with just the detrital fraction and not the organic matter (Dill, 1986), high
300 V/Cr values (>2) are indicative of anoxic conditions. Both Ni and Co are found in
301 pyrite (in addition to the occurrence of Ni in porphyrins), but high Ni/Co values are
302 associated with anoxic conditions (Jones and Manning, 1994). The relationship
303 between these ratios and depositional redox conditions are summarised in Table 1.

304 The abundances of Ni, Co, V, Cr and TOC for all samples from Robin Hood's
305 Bay and the Exshaw Formation, are presented in Table 2. Both the Ni/Co and V/Cr
306 indices for Robin Hood's Bay show that these sediments were deposited under
307 predominantly oxic conditions. However, there is significant disagreement between
308 these ratios and the V/(V+Ni) index. Values for V/(V+Ni) range from ~0.51 – 0.89 and
309 indicate that anoxic conditions prevailed across the Sinemurian-Pliensbachian
310 boundary. Further, six samples suggest that bottom-water circulation ceased and
311 that conditions became euxinic intermittently between ~2.6 m above the boundary
312 and ~1.9 m below it (Table 2).

313 The Ni/Co ratio in the Exshaw Formation sediments ranges from 13.8 – 21.4,
314 with all four samples falling within the suboxic-anoxic parameter (Table 2). Similarly,
315 the V/(V+Ni) ratio indicates that three of the samples were deposited under suboxic-
316 anoxic conditions (SP8-10, SP10-10 and SP13-10; values of 0.67, 0.69 and 0.67,
317 respectively). However, whilst V/Cr values of 7.2 and 9.0 suggest a suboxic-anoxic
318 depositional environment for Exshaw Formation samples SP10-10 and SP13-10,

319 respectively, this ratio also yields values that are representative of dysoxic conditions
320 for samples SP8-10 and SP9-10 (2.0 and 2.1, respectively).

321 Total organic carbon content is generally low in the Sinemurian-Pliensbachian
322 sediments, varying from ~0.53 – 2.46 wt. % (Table 2; Fig. 4). The data shows only
323 slight variation prior to the boundary (~0.57 – 0.86 wt. %; Fig. 4), but an overall
324 gradual increase above the boundary (from ~0.58 – 2.46 wt. %; Fig. 4). Total organic
325 carbon values in the Exshaw Formation samples range from 1.2 – 11 wt. %.

326

327 *5.2 Nickel stable isotopes*

328 New Ni stable isotope data for a select suite of the organic-rich sediments at
329 Robin Hood's Bay is presented (see Table 3). From the base of Bed 71 the sampling
330 interval for Ni isotope analysis is ~40 cm (Fig. 2). A profile of δ^{60}Ni values for the
331 section is shown alongside Ni concentration and TOC for comparison (Fig. 4).

332 The δ^{60}Ni of these samples is extremely variable, ranging from 0.28 ± 0.05 –
333 1.60 ± 0.05 ‰ (Fig. 4; Table 3). Two noticeable peaks in δ^{60}Ni values are observed 0.8
334 m above and 2.1 m below the Sinemurian-Pliensbachian boundary (1.26 ± 0.05 ‰
335 and 1.60 ± 0.05 ‰, respectively) that approximately correlate with the tops of beds
336 70 and 74. The greatest range in δ^{60}Ni values occurs below the boundary (~1.32 ‰),
337 compared to a range of ~0.97 ‰ above the boundary (Fig. 4). In this section and
338 dataset there is no apparent relationship between the degree of Ni isotope
339 fractionation and depositional redox conditions, TOC or stratigraphic height (Fig. 4).

340 Nickel stable isotope data for the Exshaw Formation is also presented in
341 Table 3. The δ^{60}Ni values in these samples range from 0.46 ± 0.04 to 2.50 ± 0.04 ‰
342 (Table 3). As with the Robin Hood's Bay section, no relationship exists between δ^{60}Ni

and sample depth or between δ^{60}Ni and depositional redox conditions, TOC or stratigraphic position (Fig. 4).

6. Discussion

6.1. Evaluating the suitability of V/(V+Ni) as a redox proxy: How applicable is it?

The Ni/Co and V/Cr redox indices are recommended by a number of workers as the most reliable of the paleo-environmental proxies (eg. Jones and Manning, 1994; Rimmer, 2004), and have been used by several studies to provide accurate and consistent evaluations of paleoredox conditions at the time of sediment deposition (eg. Rimmer, 2004; Selby et al., 2009; this study). However, this study finds that there is significant disagreement between these indices and the V/(V+Ni) index. For Robin Hood's Bay, the latter index suggests that the sediments were deposited in predominantly suboxic-anoxic bottom-waters, with intermittent euxinic periods. However, both the V/Cr and Ni/Co ratios indicate that the Robin Hood's Bay samples were deposited under largely oxic condition. Such disparity between the redox indices is also noted by both Rimmer (2004) and Selby et al. (2009), who observe that the V/(V+Ni) index suggests suboxic-anoxic conditions for sediments otherwise indicated to have been deposited under oxic conditions by the V/Cr and Ni/Co ratios.

Preliminary work by Lewan and Maynard (1982) and Lewan (1984) suggested that redox potential was a dominant control on the wide range of V/(V+Ni) values observed in petroleum source rocks and oils. Following this, Hatch and Leventhal

(1992) were the first to develop and utilise the V/(V+Ni) index as a measure of relative redox potential in organic-rich sediments. Their study focused on applying this index specifically to marine black shales in the Pennsylvanian Stark Shale Member of the Dennis Limestone, Wabaunsee County, Kansas, USA (Hatch and Leventhal, 1992). Therefore, the ranges they defined for the V/(V+Ni) ratio and the associated redox conditions (summarised in Table 1), are applicable to this specific geological basin and are sensitive to localised geochemical variations therein.

Hatch and Leventhal (1992) show that for the Stark Shale Member, with the exception of two outliers, low TOC values (<2.5 wt. %) correspond to V/(V+Ni) values <0.75, and samples containing greater TOC (>7.5 wt. %) have corresponding higher V/(V+Ni) values (0.75; Fig. 5). However, this relationship is not observed in the majority of the Sinemurian-Pliensbachian or Exshaw Formation sediments, with samples containing low TOC providing a range in V/(V+Ni) data from ~0.33 – 0.89. This immediately indicates that there are significant geochemical differences between these three geological sites. This may be due to differences in both geological age and stratigraphy, with the Stark Shale Member (Late Carboniferous) being a darker grey, non-sandy shale with higher TOC content (Hatch and Leventhal, 1992). As such, this comparison suggests that the redox index V/(V+Ni), originally developed for a specific geological basin, may not be applicable to other geological sites, particularly those that possess differing geological and geochemical characteristics. Factors that may have a profound effect upon the applicability of such a threshold from one study to another include: differences in the influx of nutrients and trace elements, type and relative amounts of organic matter, and degrees of oceanic mixing (eg. Rimmer, 2004). However, these are preliminary

findings from a small dataset and further investigation is recommended. In agreement with Rimmer (2004), this study therefore suggests that caution should be taken when applying redox indices established by other studies for single geological sites.

6.2. Nickel stable isotope fractionation in marine sediments

Nickel stable isotope data for the Exshaw Formation and the Sinemurian-Pliensbachian GSSP is presented in Table 3 and Figure 6, and is the first to be obtained for a suite of organic-rich marine sediments. The Exshaw Formation shales define a realm of δ^{60}Ni values of 0.46 ± 0.04 to 2.50 ± 0.04 ‰ (a range of ~2.04 ‰; Fig. 6). This range overlaps with, and is comparable to the δ^{60}Ni data for the Sinemurian-Pliensbachian boundary GSSP (0.28 ± 0.05 to 1.60 ± 0.05 ‰; ~1.32 ‰; Fig. 6). Although there are currently no estimations for the Ni isotopic composition of the palaeo-ocean, the present-day global seawater δ^{60}Ni value has been constrained as 1.44 ± 0.15 ‰ (Cameron and Vance, 2014). This value lies within the δ^{60}Ni range of the marine sediments (Fig. 6; this study). Draw-down of Ni through the water column does not induce isotopic fractionation, and as such, the Ni stable isotope composition of the ocean is assumed to be homogenous (Cameron and Vance, 2014). However, the Ni stable isotope composition of the organic-rich sediments is far from homogenous, with δ^{60}Ni values that are either significantly lighter or heavier than the present-day seawater δ^{60}Ni value (Fig. 6). Assuming that global ocean homogeneity has persisted throughout geological time, the fractionation observed in the marine sediments must therefore be recording the

415 substantially variable isotopic compositions of the sources of dissolved Ni into the
416 oceans.

417 This preliminary study presents Ni isotope and Ni concentration data from
418 bulk sample analysis. To assess what fraction of the selected metals may be
419 authigenic versus lithogenic, Table 4 presents Ni concentration data from this study,
420 and from average shale and average upper continental crust. It is clear from this that
421 the authigenic contribution of Ni in these samples is < 50 % (Table 4), suggesting that
422 > 50 % of the sample is represented by the lithogenic fraction.

423 For both sample sets, no correlation is observed between δ^{60}Ni and Ni
424 abundance, indicating that the level of Ni isotope fractionation in bulk marine
425 sediments here is not directly controlled by the degree of Ni enrichment. Similarly,
426 no relationship exists between δ^{60}Ni and redox for either sample set, suggesting that
427 the level of isotopic fractionation is not solely dictated by the bottom water redox
428 conditions at the time of sediment deposition. However, although it is currently
429 poorly understood, it is interesting to consider whether or not the degree of organic
430 matter preservation could have an effect on the observed isotopic fractionation
431 within the sediments. The samples used for Ni isotope analysis across the
432 Sinemurian-Pliensbachian boundary were deposited in predominantly oxic
433 conditions (using the Ni/Co and V/Cr ratios). The tetrapyrrole complexes known to
434 hold the majority of Ni in organic matter are poorly preserved under these
435 conditions (Lewan and Maynard, 1982). As such, assuming break down of these
436 complexes is heterogeneous, and that it does not result in the preferential loss of a
437 particular isotope of Ni, this lack of preservation may at least partially contribute to
438 the observed Ni isotope fractionation in these sediments.

In addition, no correlation is seen between δ^{60}Ni and TOC concentration in these samples, indicating that Ni isotope fractionation is not dependent on the concentration of organic matter in these sediments. However, all samples in this study have TOC contents of <3.0 wt. % (Table 3; apart from Exshaw Fm. sample SP10-10; 11.05 wt. %). As such, to further investigate the relationship between Ni fractionation and the organic carbon reservoir, work should be conducted on samples containing more varied and greater levels of TOC.

6.3. Fractionation of nickel stable isotopes in marine organic-rich sediments vs. terrestrial samples, extra-terrestrial samples and ferromanganese crusts

Marine sediments from the Exshaw Formation and Sinemurian-Pliensbachian GSSP yield a comparable range in δ^{60}Ni values (0.5-2.5 ‰ and 0.3-1.6 ‰, respectively; Fig. 6). Figure 6 compares these Ni isotopic values with that of bulk Earth and extraterrestrial samples (Cameron et al*.,* 2009), including meteorites (0.2 ‰ to 0.4 ‰), basalts (0 to 0.3 ‰) and continental sediments (0 to 0.2 ‰). It is clear that these samples are significantly isotopically lighter than the organic-rich sediments (this study). In addition, Ni stable isotope fractionation occurs to a much greater degree in the sedimentary marine environment. Despite this though, there is minimal overlap between the δ^{60}Ni values for the organic-rich sediments and those of the abiotic terrestrial and extraterrestrial samples (Fig. 6).

The reasons for the heightened isotopic fractionation in marine sediments are currently poorly understood due to an extremely limited sample database. However, the complexity of the marine environment is likely to play a critical role in this. With assumed ocean isotopic homogeneity (Cameron and Vance, 2014), the

463 sources of dissolved Ni into seawater must exert a substantial control on the
464 observed degree of isotopic fractionation. This may be partially attributed to the
465 variability of the Ni isotope composition of the dissolved phase of rivers, which are a
466 dominant source of Ni to the global oceans (δ^{60}Ni = 0.29 to 1.34 ‰; Cameron and
467 Vance, 2014). The heavier isotope composition of this fraction relative to silicates
468 and continental sediments (0 ‰ to 0.3 ‰; Cameron et al., 2009) likely reflects
469 isotopic fractionation induced by the weathering environment during riverine
470 transport (Cameron and Vance, 2014).

471 However, this study demonstrates that the Ni isotopic composition of
472 organic-rich marine sediments (δ^{60}Ni = 0.28 to 2.50 ‰; this study) are significantly
473 heavier than that of the riverine source (average δ^{60}Ni = 0.80 ‰; Cameron and
474 Vance, 2014). This is also the case for the dissolved phase of present-day seawater
475 (δ^{60}Ni = 1.44 ± 0.15 ‰; Cameron and Vance, 2014). To reconcile this, there must
476 therefore be either an additional input that is isotopically heavier than the riverine
477 source (Cameron and Vance, 2014).

478 Dissolved trace metals are often removed from the water column via
479 adsorption to mineral surfaces as they are incorporated into the sediment. The
480 adsorption process, in particular to Mn and Fe oxyhydroxides, is known to induce
481 isotopic fraction in a number of stable isotope systems, including Mo and U
482 (Brennecka et al., 2011; Wasylenki et al., 2008; 2011). Sorption to Fe-Mn oxides is
483 the main output of Ni from the oceans (Cameron and Vance, 2014), and more
484 recently, this fractionation effect has also been revealed in the Ni stable isotope
485 system (Wasylenki et al., 2014). In addition, experiments focusing on the adsorption
486 and co-precipitation of Ni with oxyhydroxide phases (Wasylenki et al., 2014) have

487 demonstrated that isotopically light Ni is retained by these phases whilst isotopically
488 heavy Ni is mobilised. This therefore leads to an enrichment of isotopically heavy Ni
489 in the dissolved riverine load (Wasylenki et al., 2014).

490 Nickel stable isotope data for ferromanganese crusts (0.9-2.5 ‰; Gall et al.,
491 2013) shows that their isotopic composition is comparable to that of the marine
492 organic-rich sediments discussed herein. Following analysis of ferromanganese
493 crusts in proximity to hydrothermal sources, Gall et al. (2013) suggest that
494 hydrothermal fluids may have a Ni stable isotope composition of ~ 1.5 ‰. Thus
495 hydrothermal sources may be contributing to the isotopic composition noted in the
496 marine sediments herein.

497 However, both marine sediments (this study) and ferromanganese crusts
498 (Gall et al., 2013) are at least in part recording isotopic fractionation from a source
499 that is isotopically heavier than riverine and hydrothermal Ni influxes. As continental
500 weathering is a primary source of Ni to the global oceans, it is likely that weathering-
501 induced isotope fractionation could account for the isotopically heavy Ni
502 composition of organic-rich marine sediments. Further, the heavy Ni isotope
503 signature observed in these sediments may reflect the contribution of heavy
504 dissolved Ni to the oceans following retention of the lighter Ni isotopes during
505 weathering of oxyhydroxide phases (eg. Wasylenki et al., 2014). In support of this,
506 analysis of ferromanganese crusts at varying distances from the continental shelf
507 (Gall et al., 2013) demonstrates that crusts growing in proximity to a continental
508 shelf contain the heaviest Ni isotope compositions. However, although weathering
509 does affect the isotopic composition of marine sediments, the effects resulting from

additional factors such as riverine particulates and organic compounds have yet to be constrained (Cameron and Vance, 2014).

In addition, following examination of Ni isotope data from microorganisms (δ^{60}Ni = ~0.0 to -1.6 ‰; Cameron et al., 2009), it can be noted that the Ni isotope ratios in the organic-rich sediments herein (δ^{60}Ni = ~0.28 – 2.50 ‰) appear to have been driven in the opposite direction to those of the microorganisms. Whilst the causes of Ni isotope fractionation in these sediments are currently poorly understood, it appears that there is a fractionation effect associated with the Ni isotope system that may have parallels to the carbon isotope system, with the microorganisms taking up isotopically lighter Ni, thus potentially leaving behind an isotopically heavier Ni isotope signature in the sediment. Although it is impossible to draw a definitive conclusion from the current dataset, this study suggests that microorganisms and organic matter may play a key role in our understanding of Ni isotope fractionation (in a similar manner to the rhenium-osmium isotope system; Cumming et al., 2012; Harris et al., 2013) in organic-rich marine sediments, and as such, the importance of further investigation is emphasised.

7. Conclusions

This first investigation into the Ni stable isotope composition of organic-rich marine sediments from two distinct basins has yielded a number of key observations, outlined below.

1. This preliminary dataset indicates that organic-rich sediments have a Ni stable isotope composition (δ^{60}Ni) of 0.28 to 2.50 ‰.

2. No relationship is observed between the Ni stable isotope composition of the organic-rich sediments and TOC, suggesting that fractionation is not determined by changes in the organic carbon reservoir.

3. Similarly, there is no correlation between δ^{60}Ni and Ni abundance or bottom-water redox conditions, suggesting that the process of Ni uptake and enrichment at the sediment-water interface, and the degree of oxygenation in the water-column do not exert primary control on isotopic fractionation.

4. The Ni isotope composition of marine sediments is substantially heavier and isotopically distinct to those of abiotic terrestrial and extraterrestrial samples (δ^{60}N values of -0.1 to 0.3 ‰; Cameron et al., 2009).

5. Ni isotopes in marine sediments are isotopically heavier than those in present-day seawater and rivers (δ^{60}Ni = 1.44 ± 0.15 ‰ and 0.29 to 1.340 ‰, respectively; Cameron and Vance, 2014), indicating input of an isotopically heavier source of Ni to the ocean.

6. The observed range of δ^{60}N values in marine sediments is comparable to that of ferromanganese crusts (0.9 to 2.5 ‰; Gall et al., 2013). Adsorption of Ni to Fe-Mn oxyhydroxides results in the retention of isotopically light Ni and the mobilisation of isotopically heavier Ni during oxidative weathering (Wasylenki et al., 2014). Subsequently, the dissolved riverine load is enriched in heavier Ni. It is therefore probable that isotopic fractionation driven by the weathering environment plays a key role in yielding the range of δ^{60}N values that are observed in marine sediments.

7. The relatively heavy Ni stable isotope composition of marine sediments may also in part reflect influxes of dissolved Ni from hydrothermal sources (δ^{60}Ni = 1.5 ‰; Gall et al., 2013). However, further work is needed to investigate this.

The complexity of the sediment-seawater system may be the key factor that causes such enhanced levels of Ni isotope fractionation in marine sediments relative to meteorites, basalts and continental sediments. This preliminary dataset has produced some new and important data that can be the basis for further research of Ni in organic-rich marine sediments. As such, it is recommended that the relationships between Ni isotope fractionation and factors ubiquitous to the marine depositional system, such as bottom-water redox conditions, the type of organic matter present, organic matter preservation and TOC, are further explored.

Figure captions

Figure 1: Map and photograph showing the location of the Sinemurian-Pliensbachian GSSP section, Robin Hood's Bay, UK.

Figure 2: Graphic log showing the Sinemurian-Pliensbachian boundary GSSP and the relative locations of the samples analysed in this study. Samples used for Ni isotope analysis are in bold. Bed number classification taken from Hesselbo and Jenkyns (1995).

580 Figure 3: Present-day maturity map of the Exshaw Formation within Alberta, Canada
581 (modified from Creaney and Allan, 1991). Map shows the location of the thermally
582 immature, mature and overmature zones parallel to the Rocky Mountain Front, and
583 the location of the well from which the core samples used in this study originate.
584
585 Figure 4: Nickel isotope (δ^{60}Ni), Ni abundance, and TOC profiles for the Sinemurian-
586 Pliensbachian section, presented against a corresponding stratigraphic column and
587 graphic log. Black dashed line indicates the position of the Sinemurian-Pliensbachian
588 boundary. [1]Bed numbers are from Hesselbo and Jenkyns (1995).
589
590 Figure 5: Plot showing the relationship between TOC and V/(V+Ni) for the
591 Pennsylvanian Stark Shale Member samples (solid black squares) detailed in Hatch
592 and Leventhal (1992), Robin Hood's Bay sediments (hollow diamonds; this study)
593 and the Exshaw Formation shales (hollow triangles; this study). Black dashed lines
594 mark the parameters discussed in Hatch and Leventhal (1992), whereby values of >
595 2.5 wt. % TOC correspond to V/(V+Ni) values > 0.75 for the Pennsylvanian Stark
596 Shale Member.
597
598 Figure 6: Nickel stable isotope data for organic-rich marine sediments from Robin
599 Hood's Bay, UK (RHB) and the Exshaw Formation. The grey box represents the
600 average of the Ni isotope data for meteorites, basalts and continental sediments
601 (~0.2 ‰ and 1 standard deviation either side of this; Cameron et al., 2009). The
602 white circles show Ni isotope data from ferromanganese crusts (taken from Gall et
603 al., 2013).

Table 1: Previously established values for the trace element ratios and their corresponding depositional paleoredox conditions.

Table 2: Summary of trace element and TOC data and the associated ratios used for paleoredox proxies, for the Robin Hood's Bay and Exshaw Formation marine sediments.

Table 3: New nickel stable isotope data for a selection of Robin Hood's Bay and Exshaw Formation marine sediments.

Table 4: A summary of elemental data for average shale, average upper continental crust, Robin Hood's Bay and Exshaw Formation marine sediments.

References

Alberdi, M., and Lafargue, E., 1993, Vertical variations of organic matter content in Guayuta Group (upper Cretaceous), Interior Mountain Belt, Eastern Venezuela: Organic Geochemistry, v. 20, no. 4, p. 425-436.

Birck, J. L., and Lugmair, G. W., 1988, Nickel and chromium isotopes in Allende inclusions: Earth and Planetary Science Letters, v. 90, no. 2, p. 131-143.

Brennecka, G. A., Wasylenki, L. E., Bargar, J. R., Weyer, S., and Anbar, A. D., 2011, Uranium Isotope Fractionation during Adsorption to Mn-Oxyhydroxides: Environmental Science and Technology, v. 45, no. 4, p. 1370-1375.

Cameron, V., Vance, D., Archer, C., and House, C. H., 2007, Nickel stable isotopes as biogeochemical tracers, Goldschmidt Conference Abstracts, p. A141.

Cameron, V., Vance, D., Archer, C., and House, C. H., 2009, A biomarker based on the stable isotopes of nickel: Proceedings of the National Academy of Sciences, v. 106, p. 10944-10948.

651 Cameron, V., Vance, D., and Poulton, S., 2011, Nickel isotopes, BIFs and the Archean
652 oceans, Goldschmidt Conference Abstracts, Mineralogical Magazine, p. 615.
653 Cameron, V., House, C. H., and Brantley, S. L., 2012, A First Analysis of Metallome
654 Biosignatures of Hyperthermophilic Archea: Archea, v. 2012, p. 1-12.
655 Cameron, V., and Vance, D., 2014, Heavy nickel isotope compositions in rivers and
656 the oceans, Geochimica et Cosmochimica Acta, v. 128, p. 195-211.
657 Caplan, M. L., and Bustin, R. M., 1998, Sedimentology and sequence stratigraphy of
658 Devonian-Carboniferous strata, southern Alberta: Bulletin of Canadian
659 Petroleum Geology, v. 46, p. 487-514.
660 Caplan, M. L., and Bustin, R. M., 1999, Palaeoceanographic controls on geochemical
661 characteristics of organic-rich Exshaw mudrocks: role of enhanced primary
662 production: Organic Geochemistry, v. 30, no. 2-3, p. 161-188.
663 Chen, J. H., Papanastassiou, D. A., and Wasserburg, G. J., 2009, A search for nickel
664 isotopic anomalies in iron meteorites and chondrites: Geochimica et
665 Cosmochimica Acta, v. 73, no. 5, p. 1461-1471.
666 Cook, D. L., Wadhwa, M., Clayton, R., Dauphas, N., Janney, P. E., and Davis, A. M.,
667 2007, Mass-dependent fractionation of nickel isotopes in meteoritic metal:
668 Meteoritics and Planetary Science, v. 42, no. 12, p. 2067-2077.
669 Creaney, S., and Allan, J., 1991, Hydrocarbon generation and migration in the
670 Western Canada sedimentary basin: Geological Society, London, Special
671 Publications, v. 50, no. 1, p. 189-202.
672 Creaser, R. A., Sannigrahi, P., Chacko, T., and Selby, D., 2002, Further evaluation of
673 the Re-Os geochronometer in organic-rich sedimentary rocks: a test of
674 hydrocarbon maturation effects in the Exshaw Formation, Western Canada

675 Sedimentary Basin: Geochimica et Cosmochimica Acta, v. 66, no. 19, p. 3441-
676 3452.
677 Cumming, V. M., Selby, D., and Lillis, P., 2012, Re-Os geochronology of the lacustrine
678 Green River Formation: Insights into direct depositional dating of lacustrine
679 successions, Re-Os systematics and paleocontinental weathering: Earth and
680 Planetary Science Letters, v. 359-360, p. 194-205.
681 Dean, W. T., Donovan, D. T., and Howarth, M. K., 1961, The Liassic ammonite Zones
682 and Subzones of the North West European Province: Bulletin of the Natural
683 History Museum, v. 4, p. 435-505.
684 Dera, G., Pucéat, E., Pellenard, P., Neige, P., Delsate, D., Joachimski, M. M., Reisberg,
685 L., and Martinez, M., 2009, Water mass exchange and variations in seawater
686 temperature in the NW Tethys during the Early Jurassic: Evidence from
687 neodymium and oxygen isotopes of fish teeth and belemnites: Earth and
688 Planetary Science Letters, v. 286, no. 1-2, p. 198-207.
689 Dewaker, K. N., Chandra, K., Arunachalam, J., and Karunasagar, D., 2000, Isotopic
690 fractionation of Ni60/Ni61 in kerogen and bitumen samples: Current Science,
691 v. 79, no. 12, p. 1720-1723.
692 Dill, H., 1986, Metallogenesis of early Paleozoic graptolite shales from the
693 Graefenthal Horst (Northern Bavaria-Federal Republic of Germany):
694 Economic Geology, v. 81, p. 889-903.
695 Ellrich, J., Hirner, A., and Stärk, H., 1985, Distribution of trace elements in crude oils
696 from southern Germany: Chemical Geology, v. 48, no. 1-4, p. 313-323.

697 Frausto da Silva, J.J.R., and Williams, R.J.P., 2001, The Biological Chemistry of the
698 Elements: The Inorganic Chemistry of Life, Oxford University Press, Oxford, p.
699 436-449.
700 Gall, L., Williams, H., Siebert, C., and Halliday, A., 2012, Determination of mass-
701 dependent variations in nickel isotope compositions using double spiking and
702 MC-ICPMS: Journal of Analytical Atomic Spectrometry, v. 27, no. 1, p. 137-
703 145.
704 Gall, L., Williams, H. W., Siebert, C., Halliday, A. N., Herrington, R. J., and Hein, J. R.,
705 2013, Nickel isotopic compositions of ferromanganese crusts and the
706 constancy of deep ocean inputs and continental weathering effects over the
707 Cenozoic: Earth and Planetary Science Letters, v. 375, p. 148-155.
708 Gradstein, F. M., Ogg, J. G., Schmitz, M .D., and Ogg, G. M. 2012. The Geologic Time
709 Scale 2012. Elsevier.
710 Harris, N. B., Mnich, C. A., Selby, D., and Korn, D., 2013, Minor and trace element and
711 Re-Os chemistry of the Upper Devonian Woodford Shale, Permian Basin,
712 west Texas: Insights into metal abundance and basin processes: Chemical
713 Geology, v. 356, p. 76-93.
714 Hatch, J. R., and Leventhal, J. S., 1992, Relationship between inferred redox potential
715 of the depositional environment and geochemistry of the Upper
716 Pennsylvanian (Missourian) Stark Shale Member of the Dennis Limestone,
717 Wabaunsee County, Kansas, U.S.A: Chemical Geology, v. 99, no. 1-3, p. 65-82.
718 Herzog, G. F., hall, G. S., and Brownlee, D. E., 1994, Mass fractionation of nickel
719 isotopes in metallic cosmic spheres: Geochimica et Cosmochimica Acta, v. 58,
720 no. 23, p. 5319-5323.

721 Hesselbo, S. P., and Jenkyns, H. C., 1995, A comparison of the Hettangian to Bajocian
722 successions of Dorset and Yorkshire, *in* Taylor, P. D., ed., Field Geology of the
723 British Jurassic, Geological Society, London, p. 105-150.
724 Hesselbo, S. P., Meister, C., and Grocke, D. R., 2000, A potential global stratotype for
725 the Sinemurian-Pliensbachian boundary (Lower Jurassic), Robin Hood's Bay,
726 UK: ammonite faunas and isotope stratigraphy: Geological Magazine, v. 137,
727 no. 6, p. 601-607.
728 Jones, B., and Manning, D. A. C., 1994, Comparison of geochemical indices used for
729 the interpretation of palaeoredox conditions in ancient mudstones: Chemical
730 Geology, v. 111, no. 1-4, p. 111-129.
731 Jones, C. E., Jenkyns, H. C., and Hesselbo, S. P., 1994, Strontium isotopes in Early
732 Jurassic seawater: Geochimica et Cosmochimica Acta, v. 58, no. 4, p. 1285-
733 1301.
734 Kohman, T. P., and Robison, M. S., 1980, Iron-60 as a possible heat source and
735 chronometer in the early solar system: Lunar and Planetary Science, v. 11, p.
736 564-566.
737 Konhauser, K. O., Pecoits, E., Lalonde, S. V., Papineau, D., Nisbet, E. G., Barley, M. E.,
738 Arndt, N. T., Zahnle, K., and Kamber, B. S., 2009, Oceanic nickel depletion and
739 a methanogen famine before the Great Oxidation Event: Nature, v. 458, p.
740 750-753.
741 Leenheer, M. J., 1984, Mississippian Bakken and other equivalent formations as
742 source rocks in the Western Canada basin: Organic Geochemistry, v. 6, p.
743 521-533.

744 Lewan, M. D., 1984, Factors controlling the proportionality of vanadium to nickel in
745 crude oils: Geochimica et Cosmochimica Acta, v. 48, no. 11, p. 2231-2238.
746 Lewan, M. D., and Maynard, J. B., 1982, Factors controlling enrichment of vanadium
747 and nickel in the bitumen of organic sedimentary rocks: Geochimica et
748 Cosmochimica Acta, v. 46, no. 12, p. 2547-2560.
749 Li, H.-Y., Schoonmaker, J., 2003, Chemical composition and mineralogy of marine
750 sediments. In: Treatise on Geochemistry. Sediments, Diagenesis, and
751 Sedimentary Rocks, v. 7, p. 1-35.
752 López, L., Lo Mónaco, S., Galarraga, F., Lira, A., and Cruz, C., 1995, VNi ratio in
753 maltene and asphaltene fractions of crude oils from the west Venezuelan
754 basin: correlation studies: Chemical Geology, v. 119, no. 1-4, p. 255-262.
755 Manning, L. K., Frost, C. D., and Branthaver, J. F., 1991, A neodymium isotopic study
756 of crude oils and source rocks: potential applications for petroleum
757 exploration: Chemical Geology, v. 91, no. 2, p. 125-138.
758 Meijer, N. C., Johnston, D. I., and Fullmer, E. G., 1994, Devonian stratigraphy and
759 depositional history across Peace River Highland, west central Alberta and
760 nearby British Columbia: Geological Survey of Canada Open File 2851, p. 40
761 pp.
762 Meister, C., Aberhan, M., Blau, J., Dommergues, J.-L., Feist-Burkhardt, S., Hailwood,
763 E. A., Hart, M., Hesselbo, S. P., Hounslow, M. W., Hylton, M., Morton, N.,
764 Page, K., and Price, G. D., 2006, The Global Boundary Stratotype Section and
765 Point (GSSP) for the base of the Pliensbachian Stage (Lower Jurassic), Wine
766 Haven, Yorkshire, UK: Episodes, v. 29, no. 2, p. 93-114.

767 Morand, P., and Allègre, C. J., 1983, Nickel isotopic studies in meteorites: Earth and
768 Planetary Science Letters, v. 63, no. 2, p. 167-176.
769 Moynier, F., Blichert-Toft, J., Telouk, P., Luck, J.-M., and Albarède, F., 2007,
770 Comparative stable isotope geochemistry of Ni, Cu, Zn, and Fe in chondrites
771 and iron meteorites: Geochimica et Cosmochimica Acta, v. 71, no. 17, p.
772 4365-4379.
773 Ottley, C. J., Pearson, D. G., and Irvine, G. J., 2003, A routine method for the
774 dissolution of geological samples for the analysis of REE and trace elements
775 via ICP-MS, *in* Holland, G., and Tanner, S. D., eds., Plasma source mass
776 spectrometry: applications and emerging technologies, p. 221-230.
777 Palmer, M. R., Kenison Falkner, K., Turekian, K. K., and Calvert, S. E., 1988, Sources of
778 osmium isotopes in manganese nodules: Geochimica et Cosmochimica Acta,
779 v. 52, no. 5, p. 1197-1202.
780 Peucker-Ehrenbrink, B., and Hannigan, R. E., 2000, Effects of black shale weathering
781 on the mobility of rhenium and platinum group elements: Geology, v. 28, no.
782 5, p. 475-478.
783 Piggott, N., and Lines, M. D., 1992, A case study of migration from the West Canada
784 Basin, *in* England, W. A., and Fleet, A. J., eds., Petroleum Migration, Volume
785 59, Geological Society Special Publication, p. 207-225.
786 Powell, J. H., 1984, Lithostratigraphical nomenclature of the Lias Group in the
787 Yorkshire Basin: Proceedings of the Yorkshire Geological Society, v. 45, p. 51-
788 57.
789 Quitté, G., Meier, M., Latkoczy, C., Halliday, A.N., and Günther, D., 2006, Nickel
790 isotopes in iron meteorites–nucleosynthetic anomalies in sulphides with no

791 effects in metals and no trace of ^{60}Fe: Earth and Planetary Science Letters, v.
792 242, p. 16-25.
793 Quitté, G., and Oberli, F., 2006, Quantitative extraction and high precision isotope
794 measurements of nickel by MC-ICPMS: Journal of Analytical Atomic
795 Spectrometry, v. 21, p. 1249-1255.
796 Richards, B. C., and Higgins, A. C., 1988, Devonian-Carboniferous beds of the Palliser
797 and Exshaw formations at Jura Creekm Rocky Mountains, southwestern
798 Alberta, *in* McMillan, N. J., ed., Devonian of the world, Canadian Society of
799 Petroleum Geologists Memoir, Volume 14, p. 399-412.
800 Richards, B. C., Mamet, B. L., and Bamber, E. W., 1999, Uppermost Devonian and
801 Carboniferous sequence stratigraphy, biostratigraphy and basin
802 development, Banff region, southwestern Alberta, XIV International Congress
803 on the Carboniferous and Permian, Field Trip, 4-7 and 4-17 Guidebook:
804 Calgary, Alberta.
805 Richards, C., Ross, G. M., and Utting, J., 2002, U-Pb geochronology, lithostratigraphy
806 and biostratigraphy of tuff in the Upper Famennian to Tournaisian Exshaw
807 Formation: Evidence for a mid-Paleozoic magmatic arc on the northwestern
808 margin of North America, *in* Hills, L. V., Henderson, C. M., and Bamber, E. W.,
809 eds., Carboniferous and Permian of the World: XIV ICCP Proceedings, Volume
810 19, Can Soc Petrol Geol Mem, p. 158-207.
811 Rimmer, S. M., 2004, Geochemical paleoredox indicators in Devonian-Mississippian
812 black shales, Central Appalachian Basin (USA), Chemical Geology, v. 206, no.
813 3-4, p. 373-391.

814 Rudnick, R. L., and Gao, S., 2003, 3.01 Composition of the Continental Crust: Treatise
815 on Geochemistry, v. 3, p. 1-64.
816 Schovsbo, N. H., 2001, Why barren intervals? A taphonomic case study of the
817 Scandinavian Alum Shale and its faunas: Lethaia, v. 34, no. 4, p. 271-285.
818 Sclater, F., Boyle, E., Edmond, J., 1976, On the marine geochemistry of nickel: Earth
819 and Planetary Science Letters, v. 31, p. 119-128.
820 Selby, D., and Creaser, R. A., 2005, Direct radiometric dating of the Devonian-
821 Mississippian time-scale boundary using the Re-Os black shale
822 geochronometer: Geology, v. 33, p. 545-548.
823 Selby, D., Mutterlose, J., and Condon, D. J., 2009, U-Pb and Re-Os geochronology of
824 the Aptian/Albian and Cenomanian/Turonian stage boundaries: Implications
825 for timescale calibration, osmium isotope seawater composition and Re-Os
826 systematics in organic-rich sediments: Chemical Geology, v. 265, no. 3-4, p.
827 394-409.
828 Sellwood, B. W., and Jenkyns, H. C., 1975, Basins and swells and the evolution of an
829 epeiric sea (Pliensbachian-Bajocian of Great Britain): Journal of the Geological
830 Society, v. 131, no. 4, p. 373-388.
831 Shimamura, T., and Lugmair, G. W., 1983, Ni isotopic compositions in Allende and
832 other meteorites: Earth and Planetary Science Letters, v. 63, no. 2, p. 177-
833 188.
834 Spath, L. F., 1923, Correlation of the Ibex and Jamesoni Zones of the Lower Lias:
835 Geological Magazine, v. 60, p. 6-11.

836 Wasylenki, L., Spivak-Birndorf, L., Howe, H., and Wells, R., 2014, Experiments reveal
837 the mechanism by which Ni isotopes fractionate in the weathering
838 environment: Goldschmidt Abstracts, 2661.
839 Wasylenki, L. E., Rolfe, B. A., Weeks, C. L., Spiro, T. G., and Anbar, A. D., 2008,
840 Experimental investigation of the effects of temperature and ionic strength
841 on Mo isotope fractionation during adsorption to manganese oxides:
842 Geochimica et Cosmochimica Acta, v. 72, p. 5997-6005.
843 Wasylenki, L. E., Weeks, C. L., Bargar, J. R., Spiro, T. G., Hein, J. R., and Anbar, A. D.,
844 2011, The molecular mechanism of Mo isotope fractionation during
845 adsorption to birnessite: Geochimica et Cosmochimica Acta, v. 75, no. 17, p.
846 5019-5031.
847 Wedepohl, K. H., 1971, Environmental influences on the chemical composition of
848 shales and clays: Physics and Chemistry of the Earth, v. 8, p. 305-333.
849 Xue, S., Herzog, G. F., Hall, G. S., Klein, J., Middleton, R., and Juenemann, D., 1995,
850 Stable nickel isotopes and cosmogenic beryllium-10 and aluminum-26 in
851 metallic spheroids from Meteor Crater, Arizona: Meteoritics, v. 30, p. 303-
852 310.

Figure 1

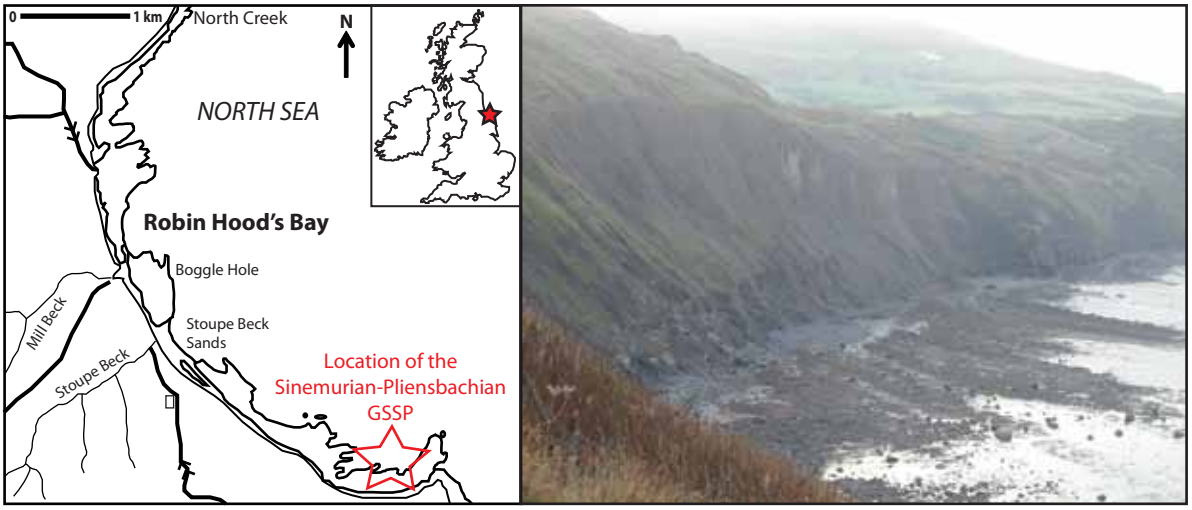
0
1 km
North Creek
N
NORTH SEA
Robin Hood's Bay
Boggle Hole
Mill Beck
Stoupe Beck
Stoupe Beck Sands
Location of the Sinemurian-Pliensbachian GSSP

Figure 2

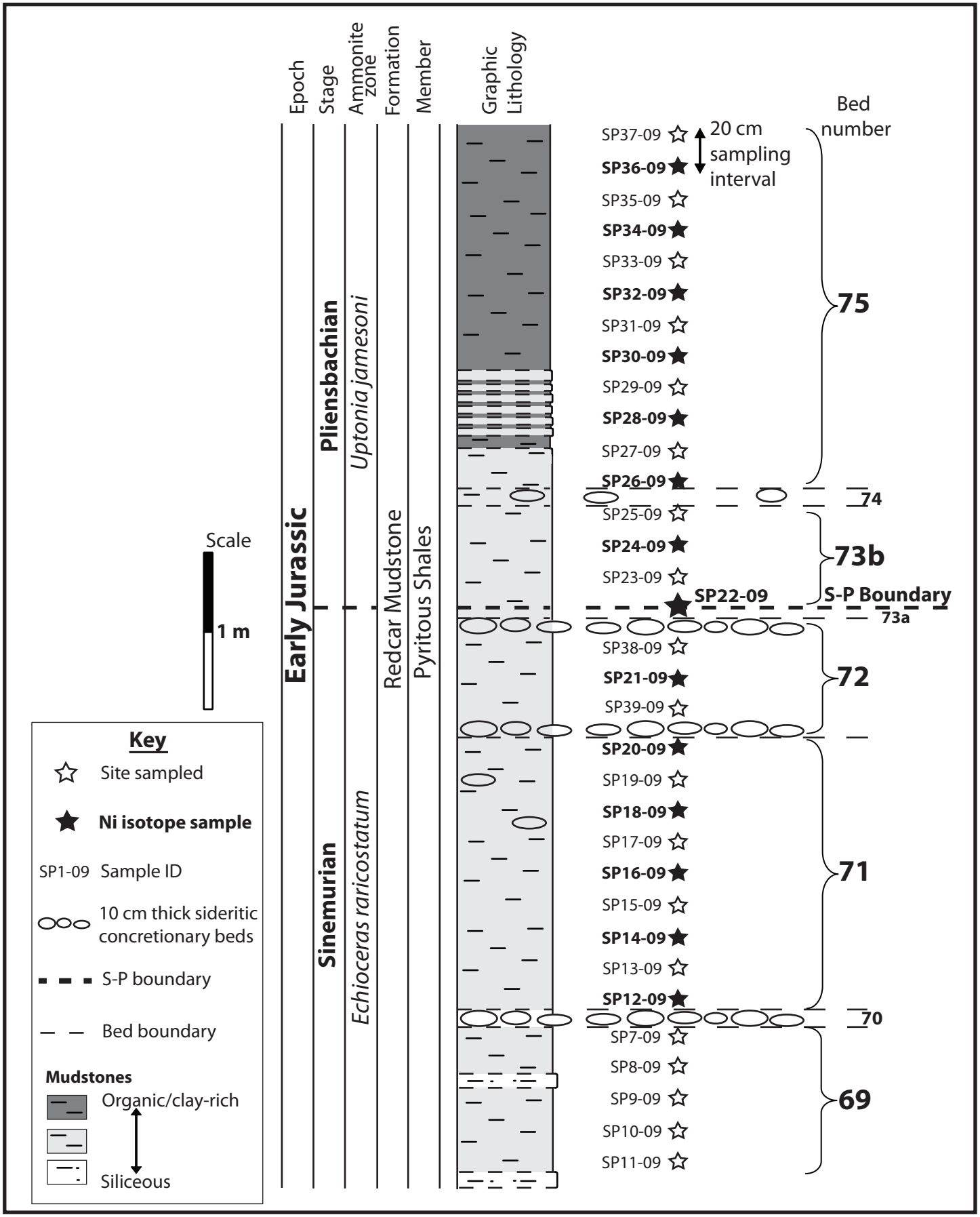
Epoch
Stage
Ammonite zone
Formation
Member
Graphic Lithology
Bed number
Early Jurassic
Pliensbachian
Sinemurian
Uptonia jamesoni
Echioceras raricostatum
Redcar Mudstone
Pyritous Shales
SP37-09
SP36-09
SP35-09
SP34-09
SP33-09
SP32-09
SP31-09
SP30-09
SP29-09
SP28-09
SP27-09
SP26-09
SP25-09
SP24-09
SP23-09
SP22-09
SP38-09
SP21-09
SP39-09
SP20-09
SP19-09
SP18-09
SP17-09
SP16-09
SP15-09
SP14-09
SP13-09
SP12-09
SP7-09
SP8-09
SP9-09
SP10-09
SP11-09
20 cm sampling interval
75
74
73b
S-P Boundary
73a
72
71
70
69
Scale
1 m
Key
Site sampled
Ni isotope sample
SP1-09 Sample ID
10 cm thick sideritic concretionary beds
S-P boundary
Bed boundary
Mudstones
Organic/clay-rich
Siliceous

Figure 3

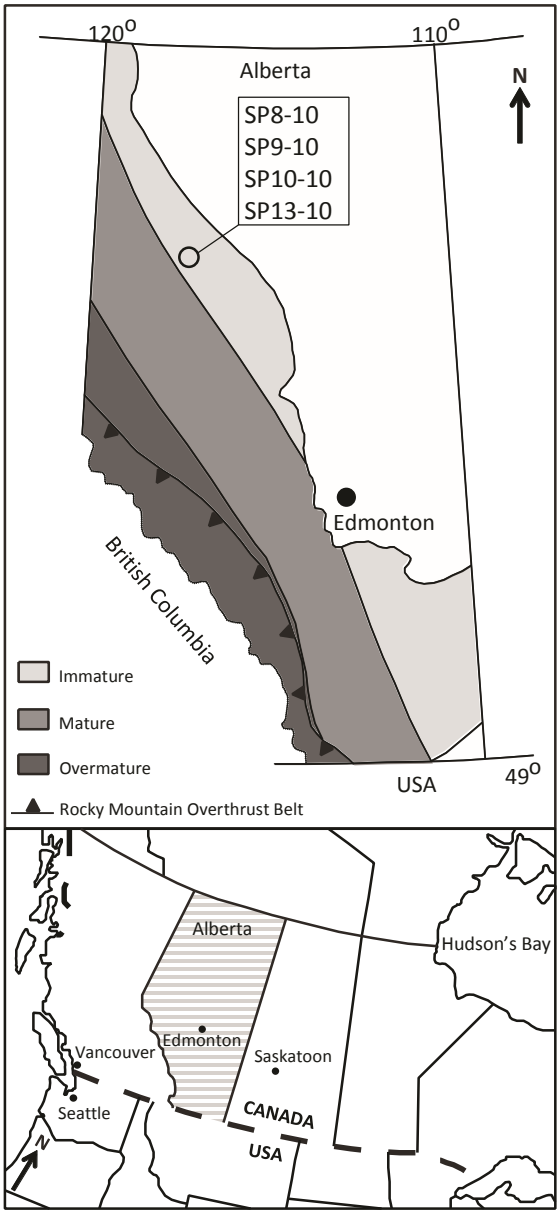
120°
110°
Alberta
N
SP8-10
SP9-10
SP10-10
SP13-10
Edmonton
British Columbia
Immature
Mature
Overmature
Rocky Mountain Overthrust Belt
USA
49°
Alberta
Hudson's Bay
Edmonton
Vancouver
Saskatoon
Seattle
CANADA
USA
N

Figure 4

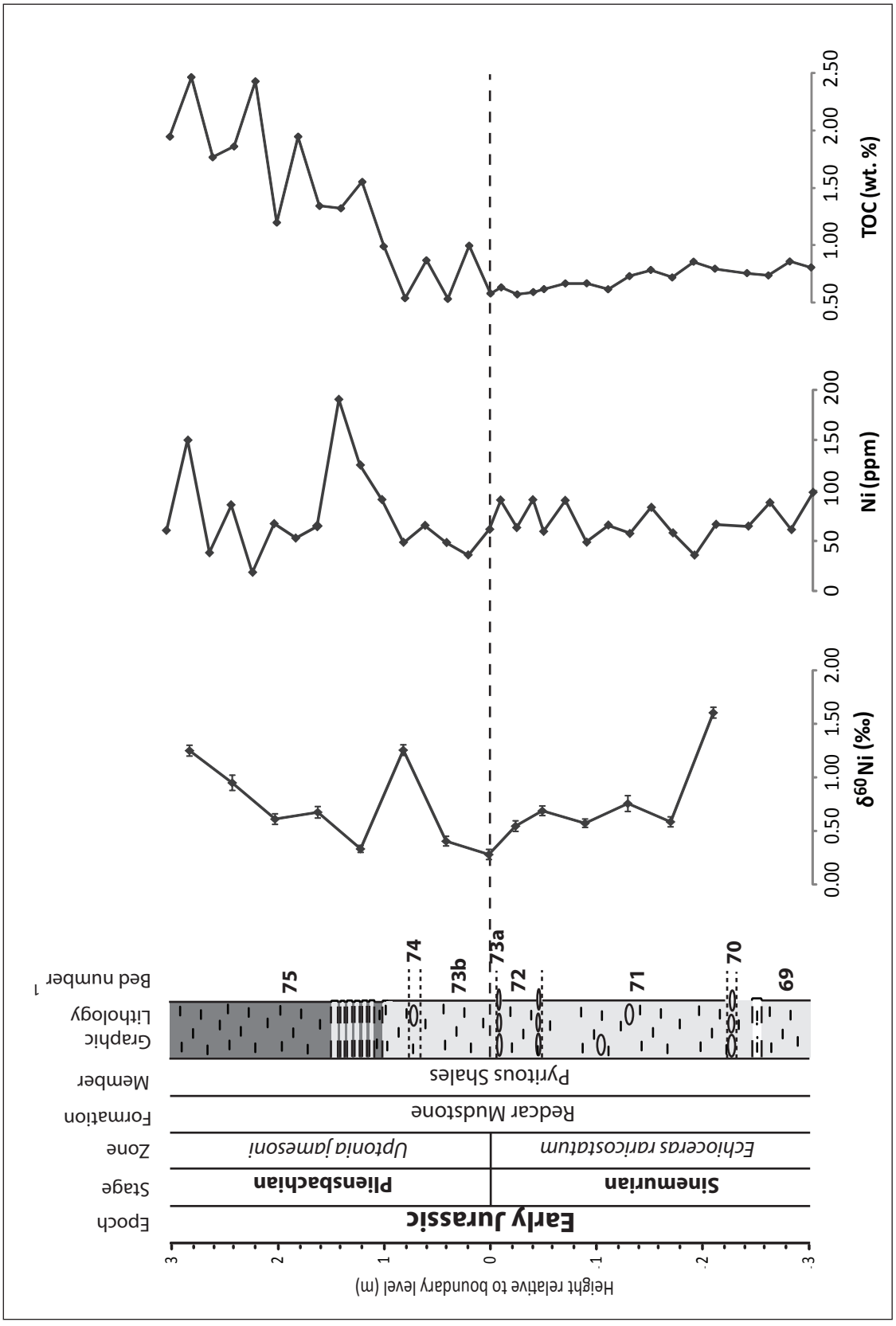
Height relative to boundary level (m)
3
2
1
0
-1
-2
-3
Epoch
Early Jurassic
Stage
Sinemurian
Pliensbachian
Zone
Echioceras raricostatum
Uptonia jamesoni
Formation
Redcar Mudstone
Member
Pyritous Shales
Graphic Lithology
Bed number
75
74
73b
73a
72
71
70
69
δ60Ni (‰)
0.00
0.50
1.00
1.50
2.00
Ni (ppm)
0
50
100
150
200
TOC (wt. %)
0.50
1.00
1.50
2.00
2.50

Figure 5

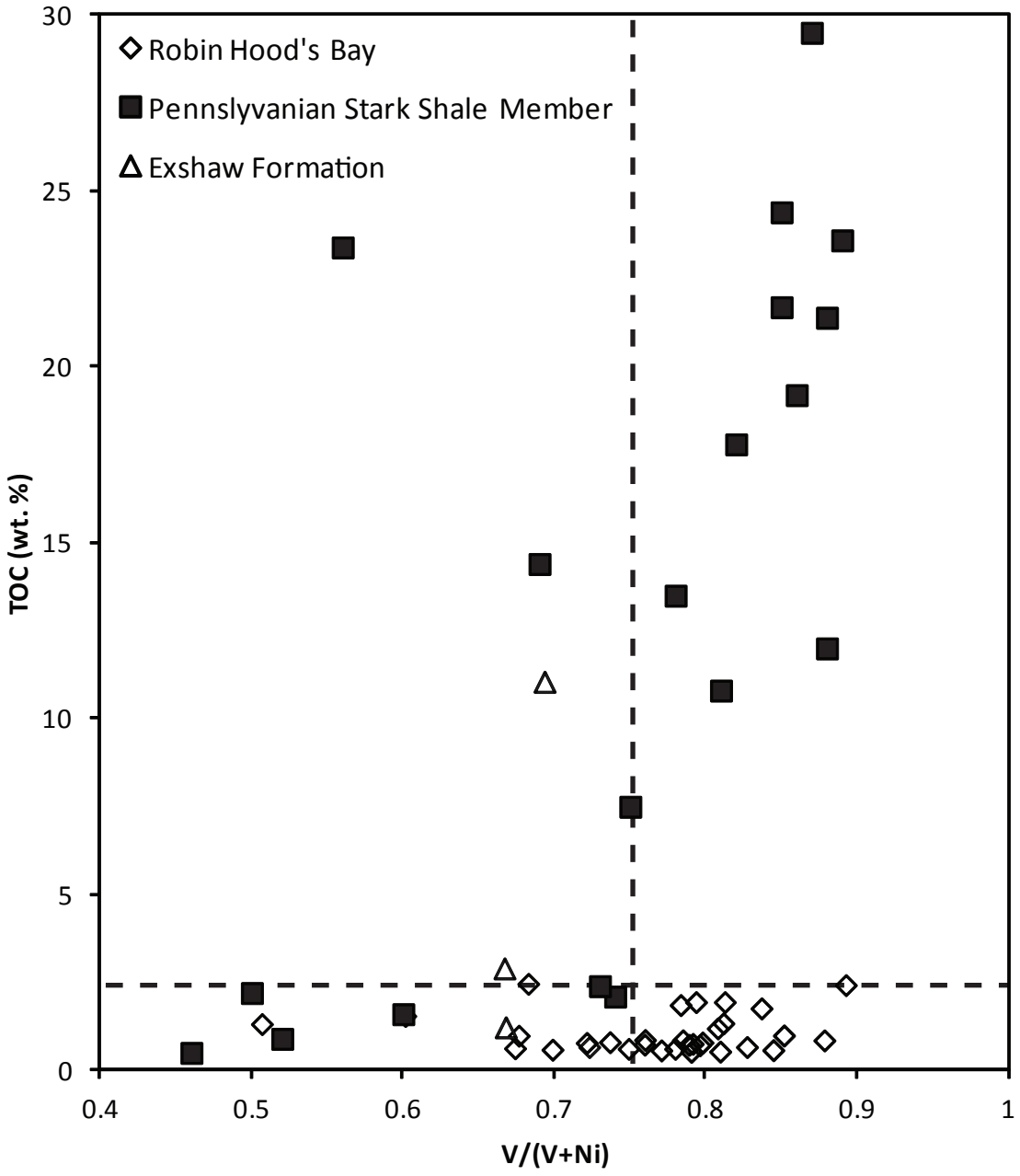
Robin Hood's Bay
Pennslyvanian Stark Shale Member
Exshaw Formation
TOC (wt. %)
V/(V+Ni)
0
5
10
15
20
25
30
0.4
0.5
0.6
0.7
0.8
0.9
1

Figure 6

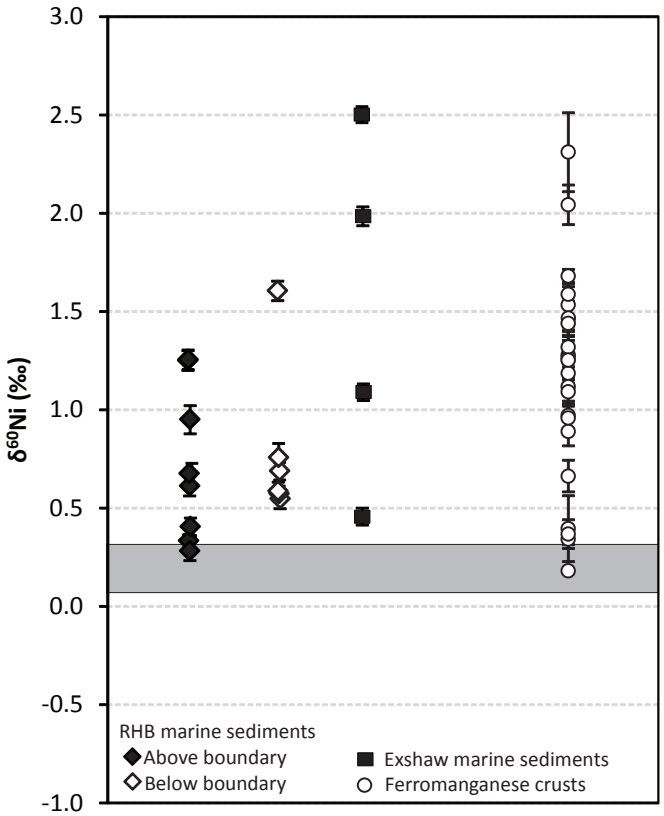
3.0
2.5
2.0
1.5
1.0
0.5
0.0
-0.5
-1.0
δ60Ni (‰)
RHB marine sediments
Above boundary
Below boundary
Exshaw marine sediments
Ferromanganese crusts

Table 1

Click here to download Table: Table 1 Redox parameters.pdf

	Oxic	Dysoxic	Suboxic-anoxic	Euxinic
V/Cr [a]	<2.00	2.00-4.25	>4.25	
Ni/Co [a]	<5.00	5.00-7.00	>7.00	
V/(V+Ni) [b]		0.46-0.60	0.54-0.82	>0.84

[a] Jones and Manning (1994)

[b] Hatch and Leventhal (1992); Schovsbo (2001)

Table 2

Click here to download Table: Table 2 Trace element data.pdf

Sample	Distance from S-P boundary (m)[a]	Depth (m)[b]	Trace elements (ppm) V	Cr	Ni	Co	Redox ratios V/Cr	Ni/Co	V/(V+Ni)	TOC (wt. %)
Robin Hood's Bay, UK										
SP37-09	3.0		230.9	130.6	60.11	26.87	1.77	2.24	0.79	1.94
SP36-09	2.8		322.4	148.2	149.9	24.70	2.18	6.07	0.68	2.46
SP35-09	2.6		194.0	107.6	37.86	18.95	1.80	2.00	0.84	1.76
SP34-09	2.4		309.3	134.5	85.57	19.82	2.30	4.32	0.78	1.86
SP33-09	2.2		152.9	107.5	18.43	12.88	1.42	1.43	0.89	2.43
SP32-09	2.0		280.8	147.3	66.81	16.21	1.91	4.12	0.81	1.20
SP31-09	1.8		227.3	130.9	52.47	20.46	1.74	2.56	0.81	1.94
SP30-09	1.6		277.7	146.9	64.49	16.37	1.89	3.94	0.81	1.34
SP29-09	1.4		195.6	158.7	190.5	20.61	1.23	9.24	0.51	1.32
SP28-09	1.2		188.8	120.2	125.2	34.40	1.57	3.64	0.60	1.55
SP27-09	1.0		189.8	148.2	90.83	21.69	1.28	4.19	0.68	0.99
SP26-09	0.8		204.9	133.4	48.25	16.55	1.54	2.92	0.81	0.54
SP25-09	0.6		205.8	130.1	65.09	22.05	1.58	2.95	0.76	0.87
SP24-09	0.4		181.1	142.6	48.06	17.63	1.27	2.73	0.79	0.53
SP23-09	0.2		204.8	120.1	35.70	19.10	1.71	1.87	0.85	0.99
SP22-09	0.0		332.6	276.8	61.23	18.45	1.20	3.32	0.84	0.58
SP38-09	-0.1		186.7	165.8	90.33	20.09	1.13	4.50	0.67	0.63
SP21-09	-0.3		211.1	122.5	62.86	20.41	1.72	3.08	0.77	0.57
SP39-09	-0.4		210.1	154.5	90.66	20.83	1.36	4.35	0.70	0.59
SP20-09	-0.5		209.2	135.9	59.13	15.35	1.54	3.85	0.78	0.62
SP19-09	-0.7		234.8	164.9	90.00	25.73	1.42	3.50	0.72	0.67
SP18-09	-0.9		231.6	142.8	48.40	18.42	1.62	2.63	0.83	0.67
SP17-09	-1.1		195.1	133.8	65.42	25.03	1.46	2.61	0.75	0.61
SP16-09	-1.3		213.1	132.0	57.04	20.22	1.62	2.82	0.79	0.73
SP15-09	-1.5		214.8	129.9	83.02	25.72	1.65	3.23	0.72	0.78
SP14-09	-1.7		225.0	133.1	57.69	17.88	1.69	3.23	0.80	0.72
SP13-09	-1.9		256.4	127.2	35.53	15.94	2.02	2.23	0.88	0.86
SP12-09	-2.1		261.0	142.8	66.18	23.19	1.83	2.85	0.80	0.79
SP8-09	-2.3		244.2	136.2	64.39	22.01	1.79	2.93	0.79	0.76
SP9-09	-2.6		277.4	140.3	87.84	21.88	1.98	4.01	0.76	0.74
SP10-09	-2.8		222.0	146.7	60.89	21.79	1.51	2.79	0.78	0.86
SP11-09	-3.0		273.9	139.0	97.97	18.88	1.97	5.19	0.74	0.81
Exshaw Formation, Canada [c]										
SP8-10		1753	108.7	53.5	3.75	54.08	2.03	14.42	0.67	1.23
SP9-10		1754	40.3	19.5	3.75	80.14	2.07	21.37	0.33	1.99
SP10-10		1756.2	350.2	38.9	11.25	154.88	9.00	13.77	0.69	11.05
SP13-10		1756.5	132.8	18.5	4.11	66.33	7.17	16.15	0.67	2.90

[a] Parameter only applicable to Robin Hood's Bay samples

[b] Parameter only applicable to Exshaw Formation samples

[c] All samples are thermally immature and from core 3-19-80-23W5

Table 3

Click here to download Table: Table 3 Ni isotope data.pdf

Sample ID	Distance from S-P boundary (m)[a]	Depth (m)[b]	δ^{60}Ni (‰)		2σ	Ni (ppm)
Robin Hood's Bay, UK						
SP36-09	2.8		1.25	±	0.05	149.92
SP34-09	2.4		0.95	±	0.07	85.57
SP32-09	2		0.61	±	0.05	66.81
SP30-09	1.6		0.67	±	0.05	64.49
SP28-09	1.2		0.33	±	0.03	125.18
SP26-09	0.8		1.26	±	0.05	48.25
SP24-09	0.4		0.40	±	0.05	48.06
SP22-09	0		0.28	±	0.05	61.23
SP21-09	-0.25		0.55	±	0.05	62.86
SP20-09	-0.5		0.69	±	0.04	59.13
SP18-09	-0.9		0.57	±	0.04	48.40
SP16-09	-1.3		0.76	±	0.07	57.04
SP14-09	-1.7		0.58	±	0.05	57.69
SP12-09	-2.1		1.60	±	0.05	66.18
Exshaw Formation, Canada [c]						
SP8-10		1753	1.09	±	0.04	54.1
SP9-10		1754	1.98	±	0.05	80.1
SP10-10		1756.2	0.46	±	0.04	154.9
SP13-10		1756.5	2.50	±	0.04	66.3

[a] Parameter only applicable to Robin Hood's Bay samples

[b] Parameter only applicable to Exshaw Formation samples

[c] All samples are thermally immature and from core 3-19-80-23W5

Table 4

Click here to download Table: Table 4 Elemental summary.pdf

Element (ppm)	Average shale[a]	Average Upper Crust[b]	This Study[c]	This study[d]
Ni	68	47	18-190	54-154
Co	19	17	3-11	12-34
V	130	97	152-332	40-350
Cr	90	92	107-268	18-53

[a] Average shale values from Wedepohl (1971)

[b] Average upper continental crust values from Rudnick and Gao (2003)

[c] Samples from Robin Hood's Bay, UK

[d] Samples from the Exshaw Formation, Canada